

AD-A097 451

TEXAS UNIV AT AUSTIN APPLIED RESEARCH LABS

F/6 17/1

SEA TEST OF A PARAMETRIC ACOUSTIC RECEIVING ARRAY AT STAGE I.(U)

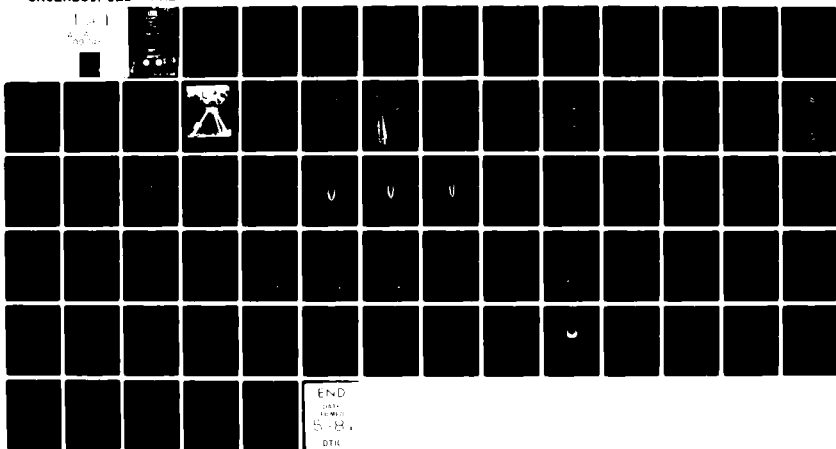
NOV 80 D F ROHDE C R CULBERTSON

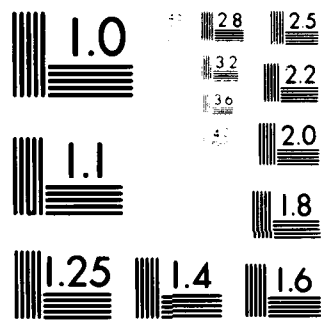
N00039-79-C-0209

UNCLASSIFIED

ARL-TR-80-37

NL





MICROCOPY RESOLUTION TEST CHART

NATIONAL BUREAU OF STANDARDS-1963-A

AD A 097451

UNCLASSIFIED

SECURITY CLASSIFICATION OF THIS PAGE (When Data Entered)

REPORT DOCUMENTATION PAGE		READ INSTRUCTIONS BEFORE COMPLETING FORM	
1. REPORT NUMBER	2. GOVT ACCESSION NO.	3. RECIPIENT'S CATALOG NUMBER	
	AD-A097451		
4. TITLE (and Subtitle)		5. TYPE OF REPORT & PERIOD COVERED	
SEA TEST OF A PARAMETRIC ACOUSTIC RECEIVING ARRAY AT STAGE I		QPR No. 3 and final report 25 Apr 79 - 15 Feb 80	
6. AUTHOR(s)		7. PERFORMING ORG. REPORT NUMBER	
David F. Rohde Robert A. Lamb C. Robert Culbertson C. Richard Reeves Tommy G. Goldsberry		ARL-TR-80-37	
8. PERFORMING ORGANIZATION NAME AND ADDRESS		9. CONTRACT OR GRANT NUMBER(s)	
Applied Research Laboratories The University of Texas at Austin Austin, Texas 78712		N00039-79-C-0289	
10. CONTROLLING OFFICE NAME AND ADDRESS		11. PROGRAM ELEMENT, PROJECT, TASK AREA & WORK UNIT NUMBERS	
Defense Advanced Research Projects Agency 1400 Wilson Blvd. Arlington, VA 22209		Item 0001	
12. MONITORING AGENCY NAME & ADDRESS (if different from Controlling Office)		13. REPORT DATE	
Naval Electronic Systems Command Department of the Navy Washington, DC 20360		7 Nov 1980	
14. SECURITY CLASS. (of this report)		15. NUMBER OF PAGES	
UNCLASSIFIED		70	
16. DISTRIBUTION STATEMENT (of this Report)		17. DECLASSIFICATION/DOWNGRADING SCHEDULE	
Approved for public release; distribution unlimited.		N/A	
18. SUPPLEMENTARY NOTES			
9. Quarterly report, no. 3 (Final) 25 Apr 79 - 15 Feb 80.			
19. KEY WORDS (Continue on reverse side if necessary and identify by block number)			
PARRAY Nonlinear acoustics Sea test Parametric reception			
20. ABSTRACT (Continue on reverse side if necessary and identify by block number)			
Applied Research Laboratories, The University of Texas at Austin, has been engaged in a program to develop an experimental parametric acoustic receiving array (PARRAY). A sea test was performed in shallow water at a site near the research platform Stage I off the coast of Florida. This report summarizes the system development, experiments performed at sea, and data analysis.			

DD FORM 1 JAN 73 1473

EDITION OF 1 NOV 65 IS OBSOLETE

UNCLASSIFIED

SECURITY CLASSIFICATION OF THIS PAGE (When Data Entered)

TABLE OF CONTENTS

	<u>Page</u>
LIST OF FIGURES	v
LIST OF TABLES	vii
I. INTRODUCTION	1
II. SEA TEST OBJECTIVES	5
III. EXPERIMENTAL PARRAY DESCRIPTION AND INSTALLATION	7
A. System Hardware	7
B. Sea Test Hardware Installation	11
IV. ANALYSIS OF EXPERIMENTS PERFORMED AT SEA	15
A. System Noise Tests	15
B. Directional Characteristics	18
1. Measured Beam Patterns from On-Line Processed Data	18
2. Theoretical Beam Patterns for Nearfield Conditions	19
3. Comparison of Theoretical Beam Patterns with Measurements	25
C. Ambient Noise	29
D. Array Gain Measurements	31
E. Signal Stability	31
F. Effects of Thermal Gradients on Propagation	33
G. Effects of Shallow Water on Parametric Reception	38
1. Introduction	38
2. Application of Normal Mode Theory to a Directional Receiver in Shallow Water	42
3. Effects of Shallow Water on the Experimental PARRAY at Stage I	45
4. Conclusions Regarding Effects of Shallow Water	49

TABLE OF CONTENTS (Cont'd)

	<u>Page</u>
V. SUMMARY AND CONCLUSIONS	51
REFERENCES	53
APPENDIX	55

Accession For	
NTIS GRA&I	<input checked="" type="checkbox"/>
DTIC TAB	<input type="checkbox"/>
Unannounced	<input type="checkbox"/>
Justification	
By	
Distribution/	
Availability Codes	
Dist	Avail and/or Special
H	

LIST OF FIGURES

<u>Figure</u>	<u>Title</u>	<u>Page</u>
1	PARRAY Functional Diagram	2
2	PARRAY Sea Test Objectives	6
3	Stage I PARRAY System Block Diagram	9
4	Photograph of PARRAY Pump In-Water Subsystem	10
5	Map of Florida Coastline Near Stage I	12
6	Long Baseline Parametric Receiving Array at Stage I, NCSC	13
7	Signal and Noise Sources in a Parametric Receiving Array (PARRAY)	16
8	PARRAY System Noise Test Results	17
9	PARRAY Beam Pattern--Stage I Sea Test	20
10	PARRAY Beam Pattern--Stage I Sea Test	21
11	PARRAY Beam Pattern--Stage I Sea Test	22
12	PARRAY Beam Pattern--Stage I Sea Test	23
13	PARRAY Geometries for Stage I Sea Test	24
14	PARRAY Beam Pattern at 319 Hz	26
15	PARRAY Beam Pattern at 543 Hz	27
16	PARRAY Beam Pattern at 731 Hz	28
17	Ambient Noise at Stage I During PARRAY Sea Test H23 Hydrophone	30
18	Comparison of PARRAY Output with Reference Hydrophone Output and Pump Frequency Acoustic Ambient Noise at Stage I	32
19	PARRAY Signal Stability Test Results	34
20	Raypath Plot for J13 Source at Middepth--Sound Speed Profile A	35
21	Raypath Plot for J13 Source at Middepth--Sound Speed Profile B	36
22	Raypath Plot for J13 Source at Middepth--Sound Speed Profile C	37
23	Raypath Plot for J15 Source Near Bottom--Sound Speed Profile A	39

LIST OF FIGURES (Cont'd)

<u>Figure</u>	<u>Title</u>	<u>Page</u>
24	Raypath Plot for J15 Source Near Bottom--Sound Speed Profile B	40
25	Raypath Plot for J15 Source Near Bottom--Sound Speed Profile C	41
26	Crossover Ranges for Low Frequency Propagation Models in 30 m Deep Water	43
27	Directional Receiver in Shallow Water	44
28	Comparison of PARRAY Half-Power Angle and Grazing Angle	48
A-1	PARRAY Functional Diagram	58
A-2	Directional Response Function of PARRAY	60
A-3	Directivity Index and Front-to-Back Ratio of the PARRAY As a Function of Acoustic Aperture in Wavelengths (L/λ)	62

LIST OF TABLES

<u>Table</u>	<u>Title</u>	<u>Page</u>
I	System Parameter Values for Experimental PARRAY at Stage I	8
II	Comparison of Measured and Theoretical Sound Pressure Level (SPL)	47

I. INTRODUCTION

Applied Research Laboratories, The University of Texas at Austin (ARL:UT), has been engaged in the design, development, and testing of an experimental parametric acoustic receiving array (PARRAY).¹⁻⁴ The PARRAY is a method of achieving highly directional reception of a low frequency acoustic wave in water using only two relatively small, high frequency transducers and some associated electronics. The PARRAY exploits the inherent nonlinearity of acoustic propagation through water to synthesize a continuous end-fire array directional characteristic without the need for a large number of hydrophones and a large quantity of beam-forming circuitry. As illustrated schematically in Fig. 1, the low frequency signal wave interacts with the high frequency pump wave to produce intermodulation products that are detected by the receiver electronics. The interaction in the volume insonified by both the pump and signal waves is such that, for the low frequency signal, an end-fire directional characteristic is produced. The PARRAY exhibits the directional characteristics of a continuous end-fire array with length equal to the pump-hydrophone separation, and thus its directivity is determined by the pump-hydrophone separation L and the target signal wavelength. A more detailed description of the PARRAY concept is presented in an appendix to this report and in the references cited in the appendix.

ARL:UT conducted a sea test of the experimental PARRAY at the Stage I offshore facility of Naval Coastal Systems Center (NCSC), Panama City, Florida, during April and May 1979. This report summarizes objectives of that sea test, the experiments performed, and analysis of the data obtained during those tests. Support for this effort has been provided by the Tactical Technology Office of Defense Advanced Research Projects Agency (DARPA) and Naval Electronic Systems Command, Code 320.

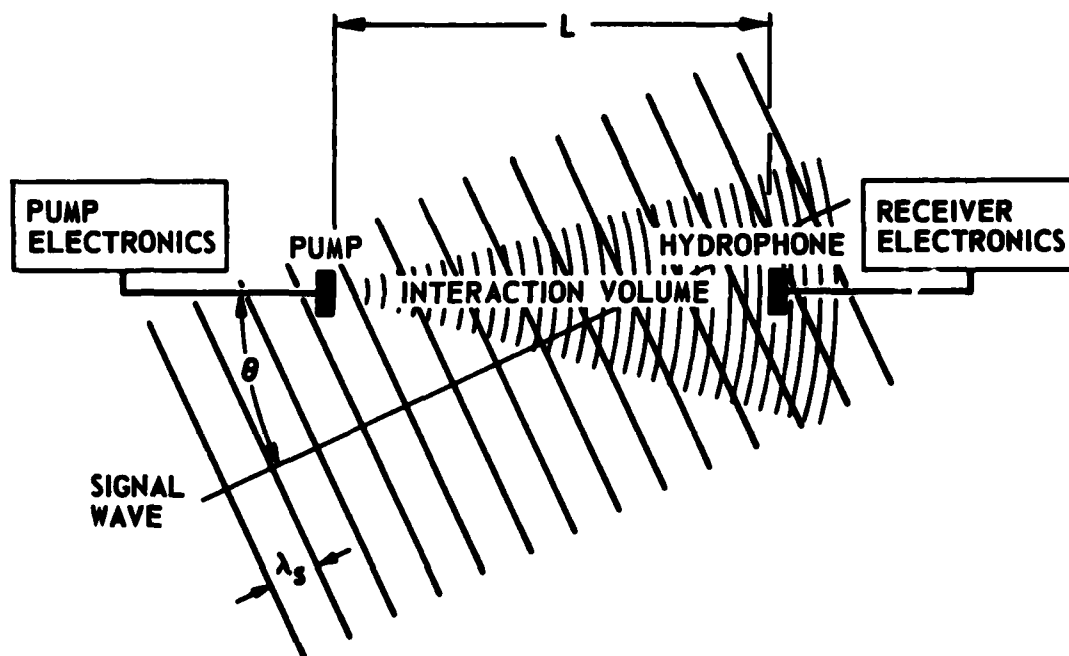


FIGURE 1
PARRAY FUNCTIONAL DIAGRAM

ARL - UT
AS-76-2102-S
DFR - DR
10 - 7 - 76

Objectives of the sea test are outlined and the approach to accomplishing these objectives is indicated in Section II.

The experimental PARRAY system is described and operating parameters of the equipment are given in Section III. The sea test schedule and installation at Stage I are also discussed in this section.

Individual tests as well as the results of these tests are reviewed in Section IV. Additional analysis to compare the measured results with theoretical predictions is discussed.

A brief summary and conclusions are given in Section V.

II. SEA TEST OBJECTIVES

The goal of the sea test was to acquire information needed to determine whether the PARRAY is a viable acoustic sensor for naval applications. The sea test provided ocean measurements which substantiated information previously obtained through analysis and lake tests by ARL:UT.²⁻⁵

The sea test objectives were:

- (1) to determine system minimum detectable level (MDL),
- (2) to verify the system model, and
- (3) to determine the effects of the medium and environment on system performance.

Each of these objectives was accomplished through a series of tests which measured not only the performance of the complete PARRAY system but also tested the subsystem hardware and measured the environmental conditions in the sea.

The relationship of each individual test to the system test objectives is depicted in Fig. 2. The tests for determination of system MDL are divided into categories relating to tests of the hardware subsystems, ambient noise measurements, and PARRAY system axial response. These same tests, plus two additional tests of directivity characteristics, are used to verify the PARRAY system model. A set of special purpose tests are used to measure factors related both to the environment and proposed deployment scenarios for the PARRAY.

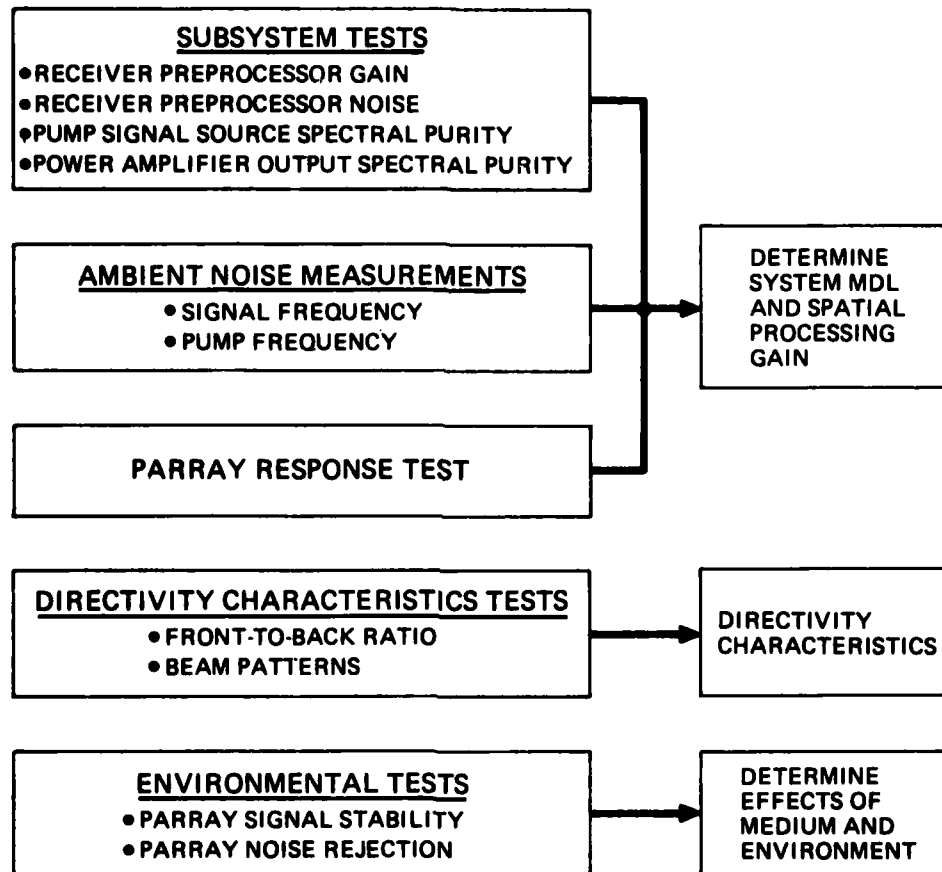


FIGURE 2
PARRAY SEA TEST OBJECTIVES

III. EXPERIMENTAL PARRAY DESCRIPTION AND INSTALLATION

A. System Hardware

System parameter values for the experimental PARRAY tested at Stage I are shown in Table I. With the exception of the pump-hydrophone separation, these are essentially the same parameter values used for the experimental PARRAY during the interim tests conducted at the Lake Travis Test Station (LTTS) of ARL:UT.²

A block diagram of the experimental PARRAY for the Stage I tests is shown in Fig. 3. The system consisted of four major units: the pump subsystem in-water hardware, the hydrophone subsystem in-water hardware, the onboard PARRAY electronic hardware, and the data processing and recording equipment.

A tripod approximately 5 m on each side provided a mounting for the following components of the pump subsystem in-water hardware: (1) the pump transducer, which projected the highly directional pump signal, (2) the tilt/scan mechanism, which allowed the pump transducer to be aligned with the PARRAY hydrophone, and (3) an ambient noise monitor (NRL/USRD reference hydrophone Type F50). A photograph of the pump subsystem in-water hardware is shown in Fig. 4. The pump transducer and associated tilt/scan mechanism are shown mounted on top of the tripod. The ambient noise monitor hydrophone can be seen attached to the leg of the tripod at the left of the photograph.

A similar tripod was used to mount the PARRAY hydrophone and tilt/scan mechanism. The PARRAY hydrophone and pump were the same size, and were constructed from the same basic design. An additional ambient noise monitor hydrophone was mounted on the hydrophone subsystem tripod

TABLE I
SYSTEM PARAMETER VALUES FOR EXPERIMENTAL PARRAY AT STAGE I

Pump Frequency	65 kHz
Receiver Electronic Noise	-151 dB re 1 V/ $\sqrt{\text{Hz}}$ for a source impedance of 15 k Ω
Power Amplifier Output	250 W
Pump Source Level	218 dB re 1 μPa at 1 m
Hydrophone Directivity Index	30 dB
Pump-hydrophone Separation	215 m
Spectrum Level SSB Noise-to-Pump Level	-165 dB

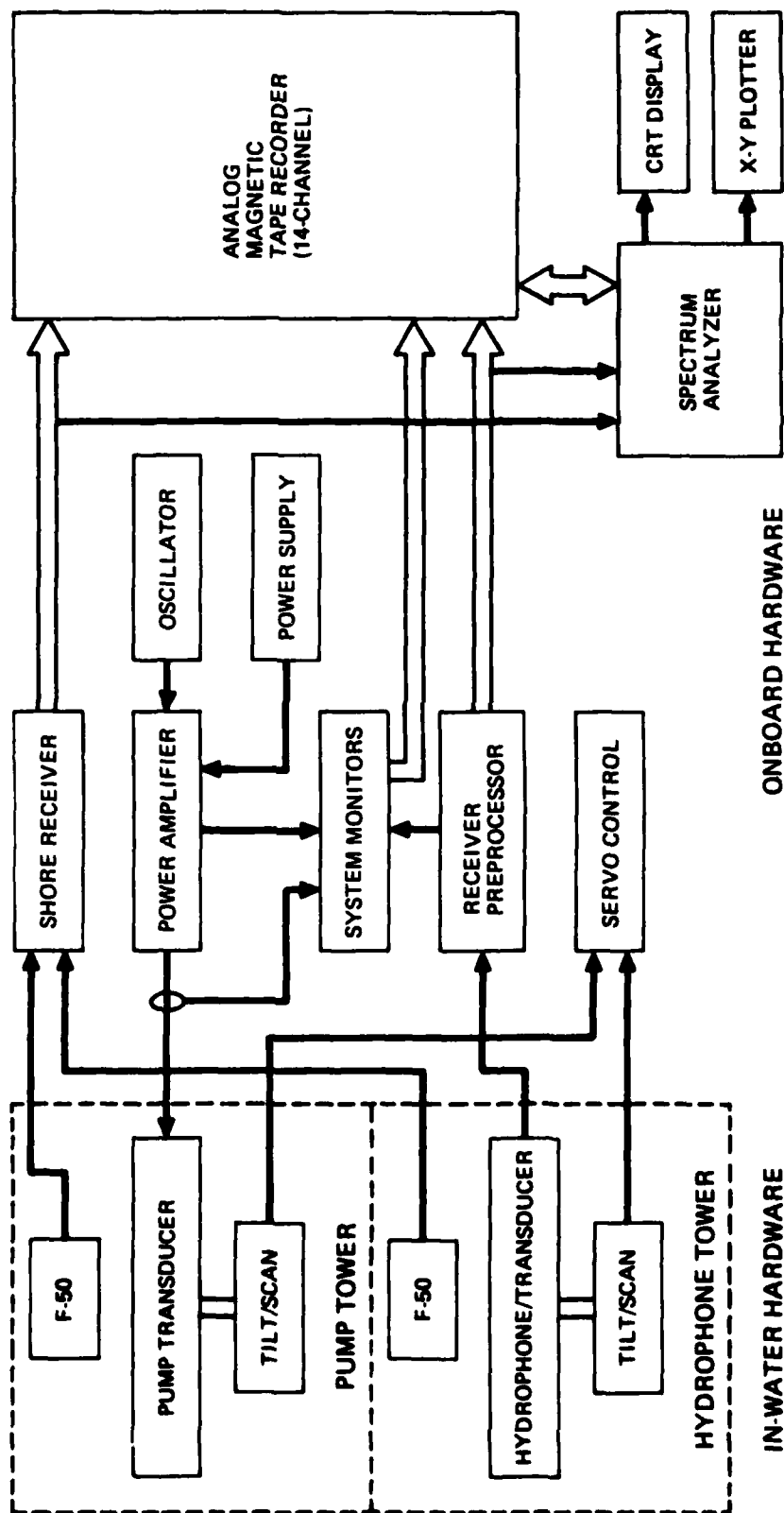


FIGURE 3
STAGE I PARRAY SYSTEM BLOCK DIAGRAM

ARL:UT
AS-78-1961
TGG - GA
11-12-80



FIGURE 4
PHOTOGRAPH OF PARRAY PUMP IN-WATER SUBSYSTEM

3524-7

to provide an additional estimate of the local ambient noise during the experiments.

The sea test PARRAY hardware was first assembled and tested at ARL:UT, both in the laboratory and at LTTS. All sensors and data channels were calibrated during March and the first two weeks of April 1979.

B. Sea Test Hardware Installation

The complete PARRAY system was shipped to NCSC on 21 April 1979. The onboard equipment was installed on Stage I during the week of 23-29 April. Bad weather delayed installation of the in-water hardware and cables until the first two days of the second week, 30 April - 1 May.

Stage I is a research platform located approximately 12 miles offshore from NCSC, Panama City, Florida, as shown in Fig. 5. The facility has a large laboratory space, which was used to house the onboard electronics.⁶ Accommodations were available on the platform, so ARL:UT personnel stayed on Stage I throughout the sea test. This permitted an intensive testing effort under a variety of weather conditions.

The PARRAY configuration for the tests at Stage I is illustrated in Fig. 6. The underwater tripods were installed in approximately 30 m of water near the platform. The tripods were separated by approximately 215 m, with the nearest one 122 m from the Stage I platform. The baseline of the PARRAY was oriented in a southwesterly direction. The transducers and tilt/scan mechanisms located on the underwater towers were connected to the onboard electronics via multiple conductor cables. Each tripod had three underwater cables: (1) PARRAY transducer, (2) F50 ambient monitor, and (3) tilt/scan control-monitor. These cables were laid back to Stage I and terminated in the electronics room.

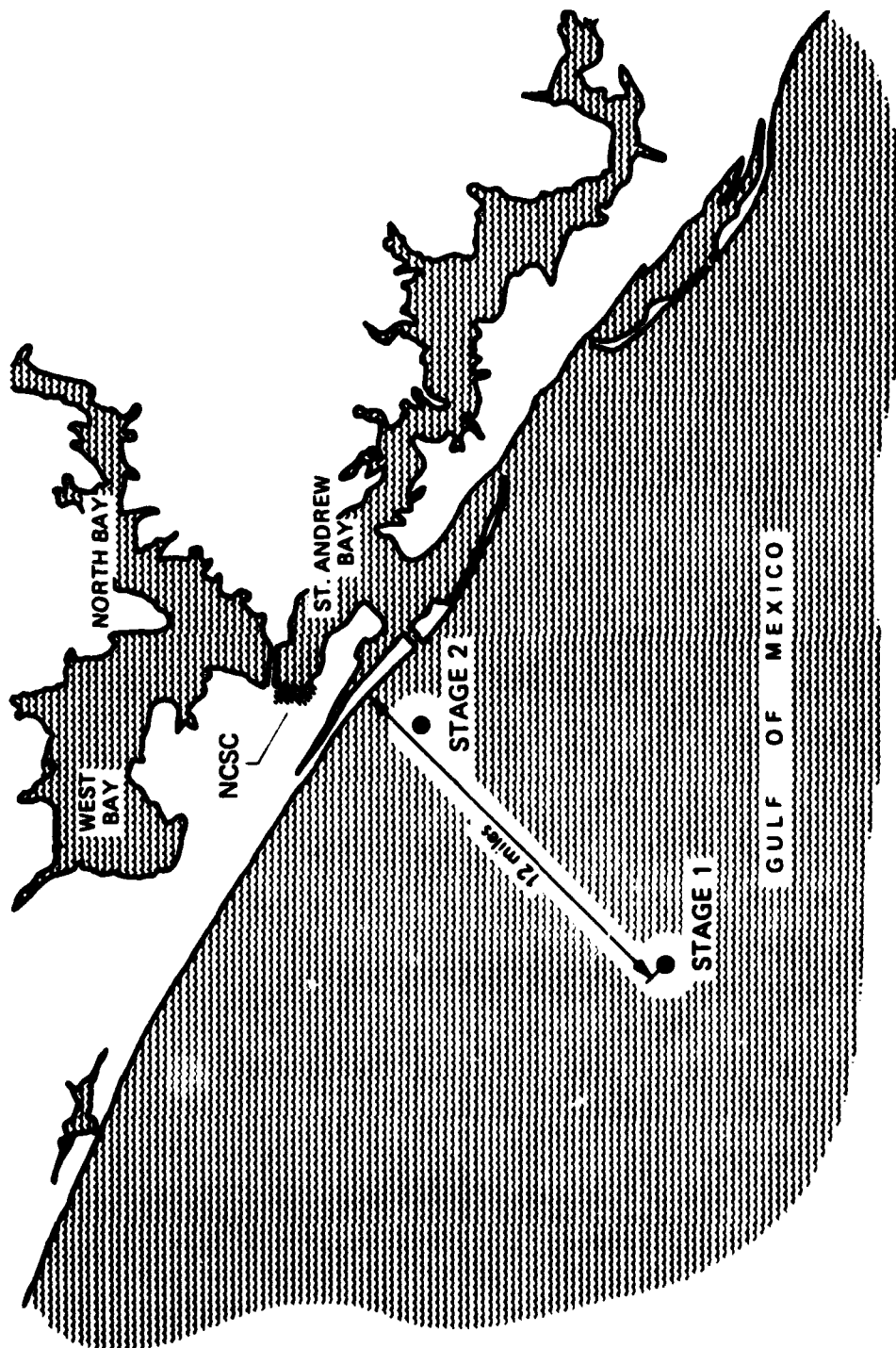


FIGURE 5
MAP OF FLORIDA COASTLINE NEAR STAGE 1

ARL UT
 AS-80-1795
 TGG - GA
 11 12 80

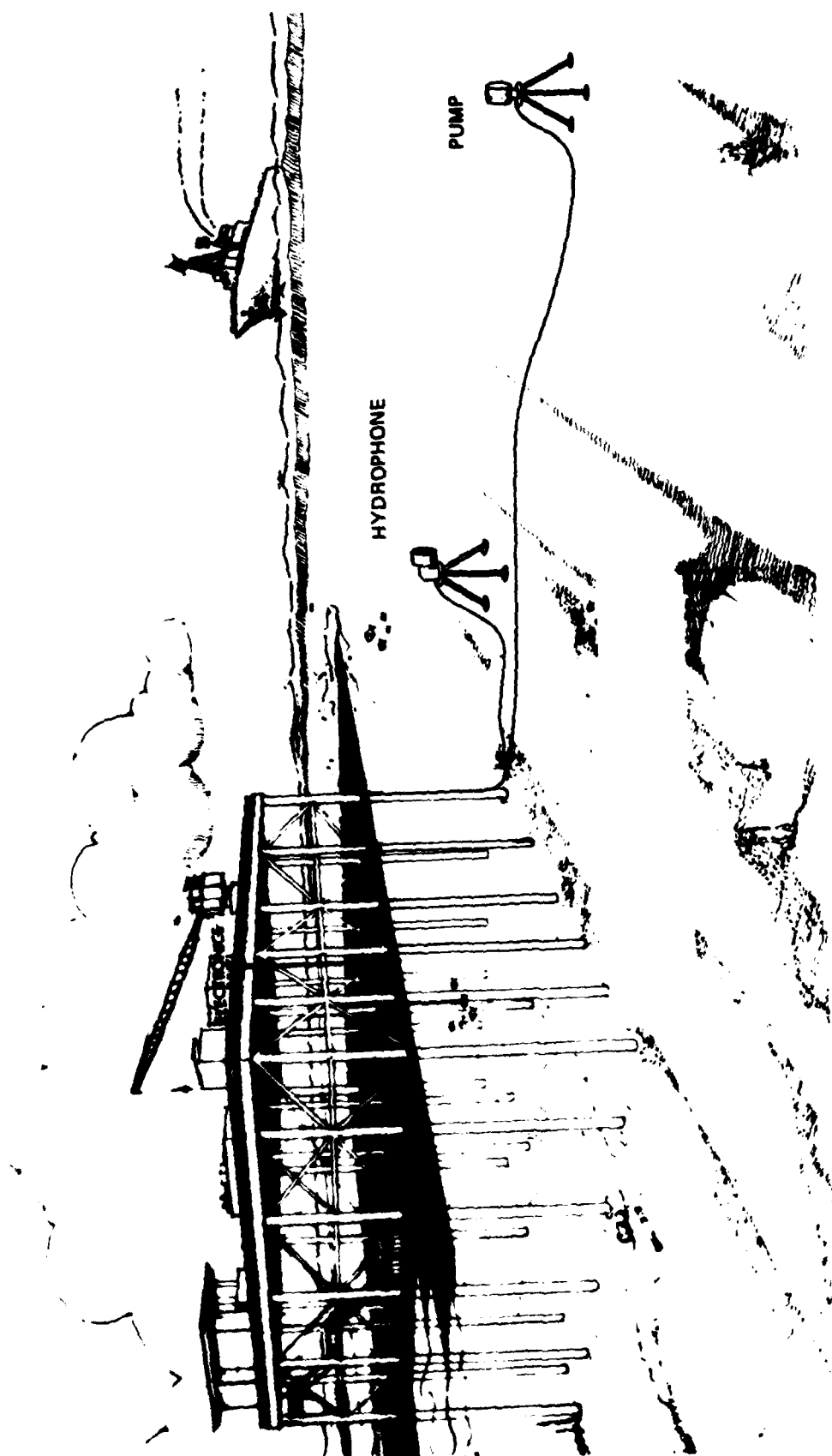


FIGURE 6
LONG BASELINE PARAMETRIC RECEIVING ARRAY AT STAGE I, NCSC

ARL:UT
AS-80-1796
TGG-GA
11-12-80

Most of the electronic hardware was located aboard Stage I. By minimizing the amount of in-water electronic hardware, the reliability of the experimental PARRAY was enhanced.

A series of experiments was performed that demonstrated proper operation of the PARRAY in the shallow water environment. The data from these experiments were used to achieve the test objectives described in the previous section of this report.

Data were obtained in two ways: (1) some data were processed on-line using a narrowband spectrum analyzer and then recorded on an x-y recorder; (2) simultaneously, additional data were recorded on multiple channel analog magnetic tape for off-line processing at a later date. The data obtained and analyzed on-line provided immediate results that were useful in conducting the experiments. Such data included measurements of system electronic noise and acoustic ambient noise, both at audio frequencies and at the pump sideband frequencies. The data recorded on analog magnetic tapes were returned to ARL:UT for analysis on the data acquisition and processing system (DAPS), used extensively in previous experiments. Analysis of data is discussed in the next section.

The system was recovered 9 May 1979 and returned to ARL:UT on 12 May 1979. All project milestones were met on time and were within the funds allocated.

IV. ANALYSIS OF EXPERIMENTS PERFORMED AT SEA

The hardware described in the previous section was used to perform a variety of experiments during the tests at Stage I. PARRAY subsystem and system noise levels were measured, as was PARRAY directional characteristics, acoustic ambient noise, array gain, and signal stability. Results of these experiments, as well as some comparisons with theoretical predictions, are given in the following subsections.

A. System Noise Tests

The parametric acoustic receiver is a complex sensor and a number of sources contribute to its noise floor, as illustrated schematically in Fig. 7. The various components of noise were isolated and measured during the experiments. The two primary components of system noise were the receiver electronic noise and the noise related to the spectral purity of the pump signal. This latter noise consisted of electronic noise from the pump oscillator, power amplifier, and power supply. These components were measured individually and in composite. The composite noise for the pump system was determined by measuring the drive current into the pump transducer, and was computed at 165 dB below the carrier, measured in a 1 Hz bandwidth at frequencies greater than 400 Hz from the pump frequency. The equivalent acoustic noise due to pump source sideband noise from 100 to 800 Hz away from the carrier is given in Fig. 8. The electronic noise has been translated through the PARRAY sensor parameters to yield an equivalent plane wave sound pressure level of approximately 35 dB re $1 \mu\text{Pa}/\sqrt{\text{Hz}}$. This pump signal sideband noise equivalent level was at least 15 dB below that of the ambient acoustic noise at Stage I in the 65 kHz pump frequency region.

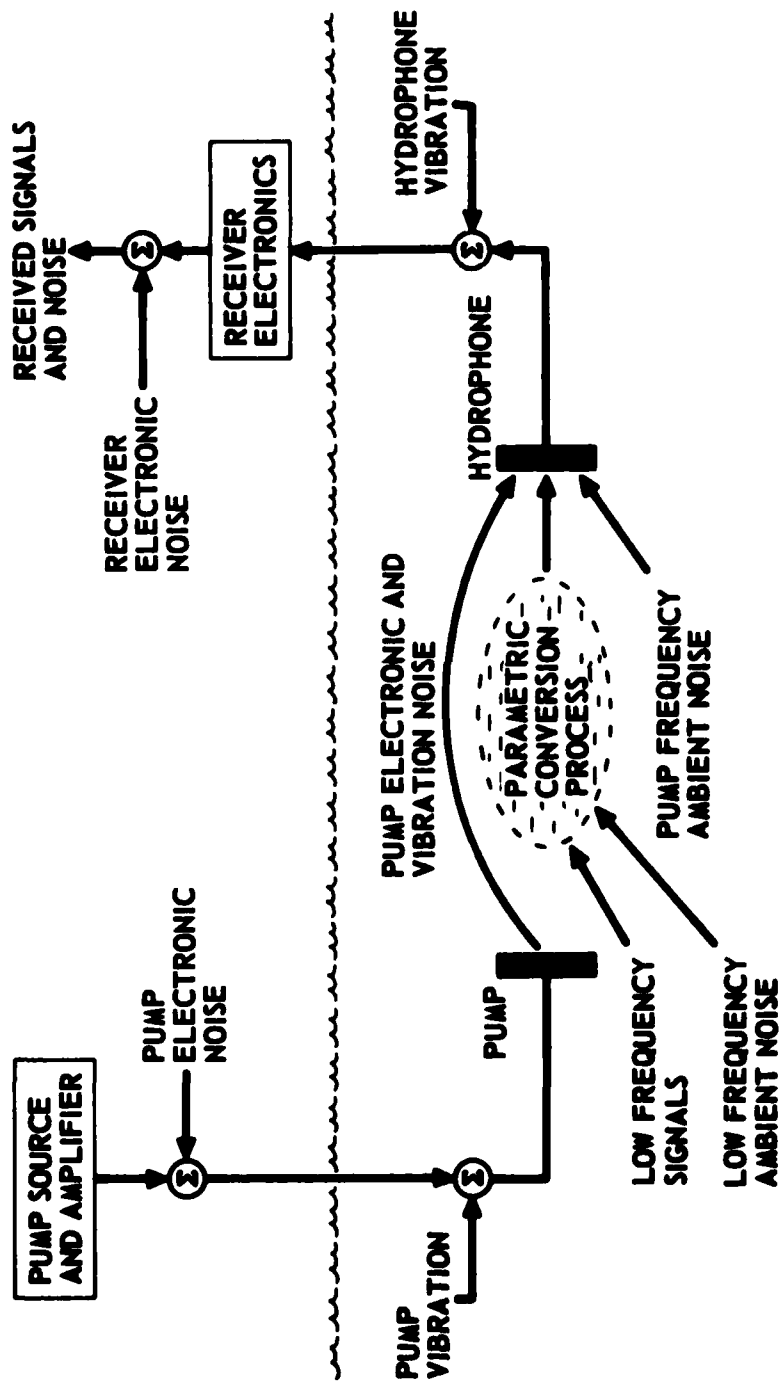


FIGURE 7
SIGNAL AND NOISE SOURCES IN A PARAMETRIC RECEIVING ARRAY (PARRAY)

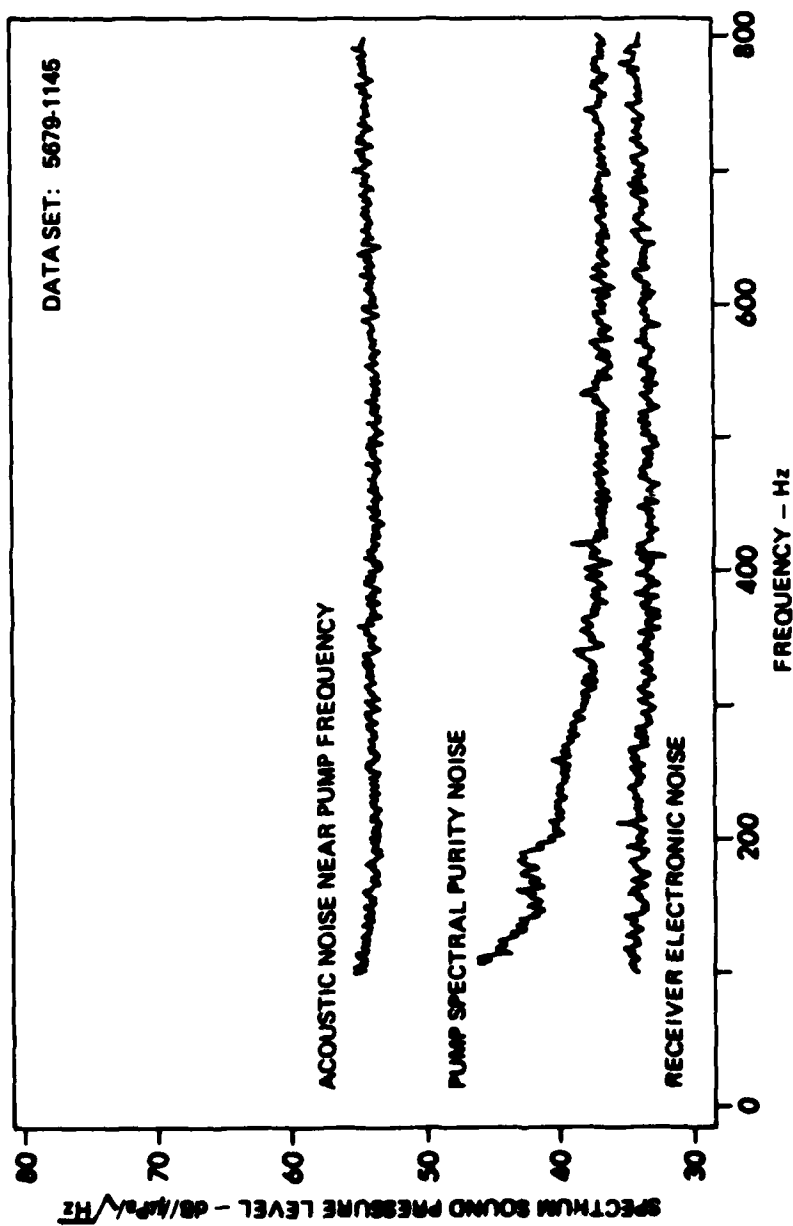


FIGURE 8
PARRAY SYSTEM NOISE TEST RESULTS

ARL:UT
AS-80-1787
TGS - GA
11-12-80

The noise from the receiver electronics was measured with and without the pump signal present. The electronic noise of the receiver was measured to be greater than 168 dB below the received pump signal level. This noise level is included in Fig. 8 as an equivalent plane wave sound pressure level. The receiver electronic noise was approximately 32 dB re $1 \mu\text{Pa}/\sqrt{\text{Hz}}$ and was nearly 20 dB below that of the ambient noise in the ocean near the 65 kHz pump frequency.

In summary, a high degree of pump spectral purity and low electronic noise levels were attained during the PARRAY sea test. The pump sideband noise and the electronic noise were of sufficiently low level so as not to contaminate the acoustic measurements.

B. Directional Characteristics

Beam patterns for the PARRAY were obtained at several frequencies. A J13 transducer suspended at a depth of 15 m from an outboard motor boat served as signal source for the beam pattern measurements. The automated tracking system from NCSC was not operational during these measurements, so a back-up system was used. Tracking was accomplished with a split-image optical range finder and a transit for bearing. The information for range and bearing from Stage I to the source boat was relayed to the tape recorder voice track by portable radio. Bearing accuracy is estimated to be $\pm 1^\circ$, with range accuracy estimated to be ± 25 m at 1000 m.

1. Measured Beam Patterns from On-Line Processed Data

Beam patterns were measured by having the source boat make a run perpendicular to the axis of the PARRAY at a constant speed and heading while the range and bearing were being recorded. A beam pattern was obtained by measuring the voltage in a 1 Hz bandwidth at the upper sideband output of the PARRAY receiver and plotting it on an x-y recorder. This was done in the field for some signal frequencies; additional beam patterns were subsequently obtained at ARL:UT from the

tape recorded data. Beam patterns for frequencies of 319 Hz and 731 Hz are shown in Figs. 9 and 10, respectively. The signal-to-noise ratio (S/N) was sufficiently high (as much as 30 dB in the main lobe) so that the beam patterns demonstrate that a well-formed beam was synthesized by the PARRAY. Selected points from the rectilinear beam patterns are replotted in polar coordinates in Figs. 11 and 12.

The data in these figures are not corrected for angle offset, axis translation, nearfield effects, or interference effects and, hence, the patterns have narrower main lobes than expected for the array length and frequency. Corrected patterns are presented in the following section and are compared with theoretical beam patterns.

2. Theoretical Beam Patterns for Nearfield Conditions

The measured beam patterns were obtained with the signal source located less than ten array lengths from the PARRAY, i.e., within the nearfield of the PARRAY. A method for evaluating the effects of near-field reception has been developed by Berkta and Shooter,⁷ and is employed in this section to obtain theoretical beam patterns for the experimental configuration used at Stage I.

For the geometrical configuration in Fig. 13(a), Berkta and Shooter have shown that the nearfield directivity function of an end-fire line array is

$$D(R, \theta) = \left(\ln \frac{R}{R-L} \right)^{-1} \int_{v_1}^{v_2} \frac{1}{v} \exp(-jv) dv, \quad (1)$$

where

$$v_1 = kR(1-\cos\theta),$$

$$v_2 = k \left[\left(R^2 + L^2 - 2LR\cos\theta \right)^{1/2} - (R\cos\theta - L) \right], \text{ and}$$

$$k = \text{acoustic wave number.}$$

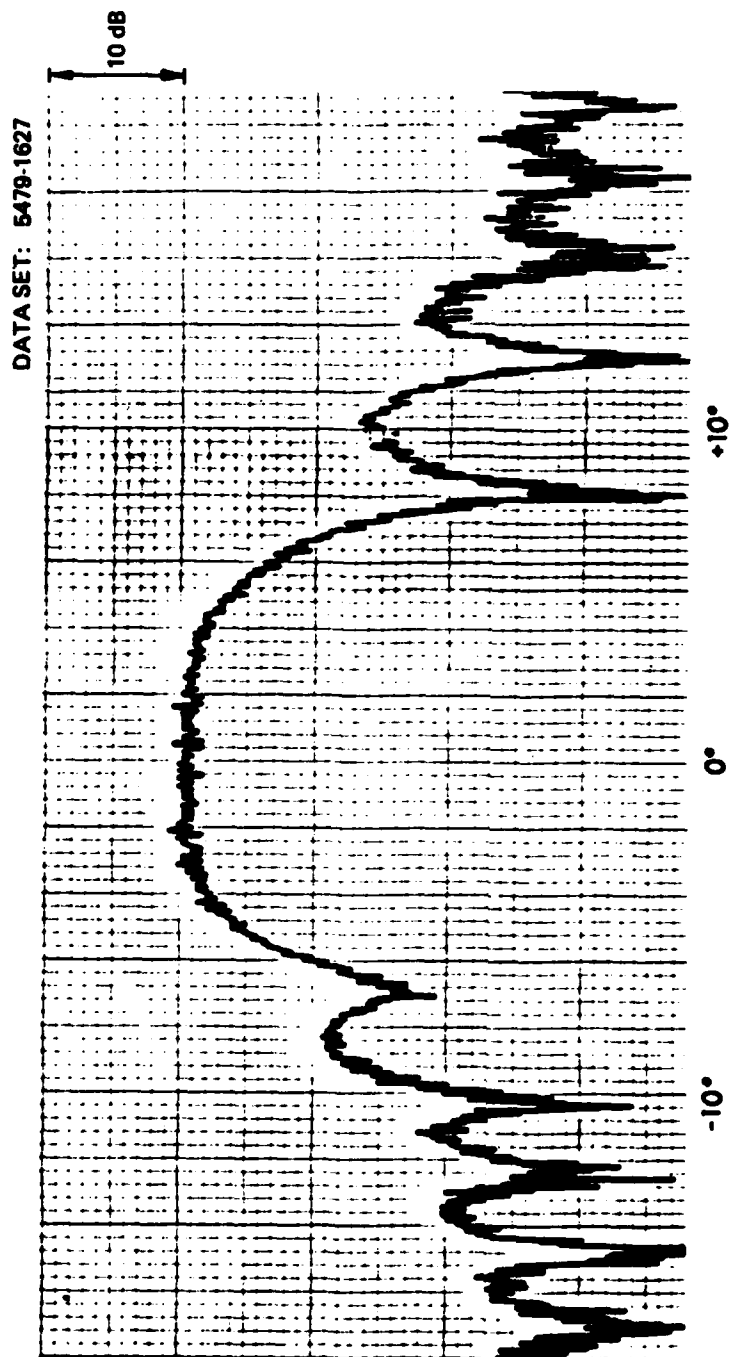


FIGURE 9
PARRAY BEAM PATTERN - STAGE I SEA TEST
 $f = 319 \text{ Hz}$

ARL:UT
AS-80-1798
TGG - GA
11-12-80

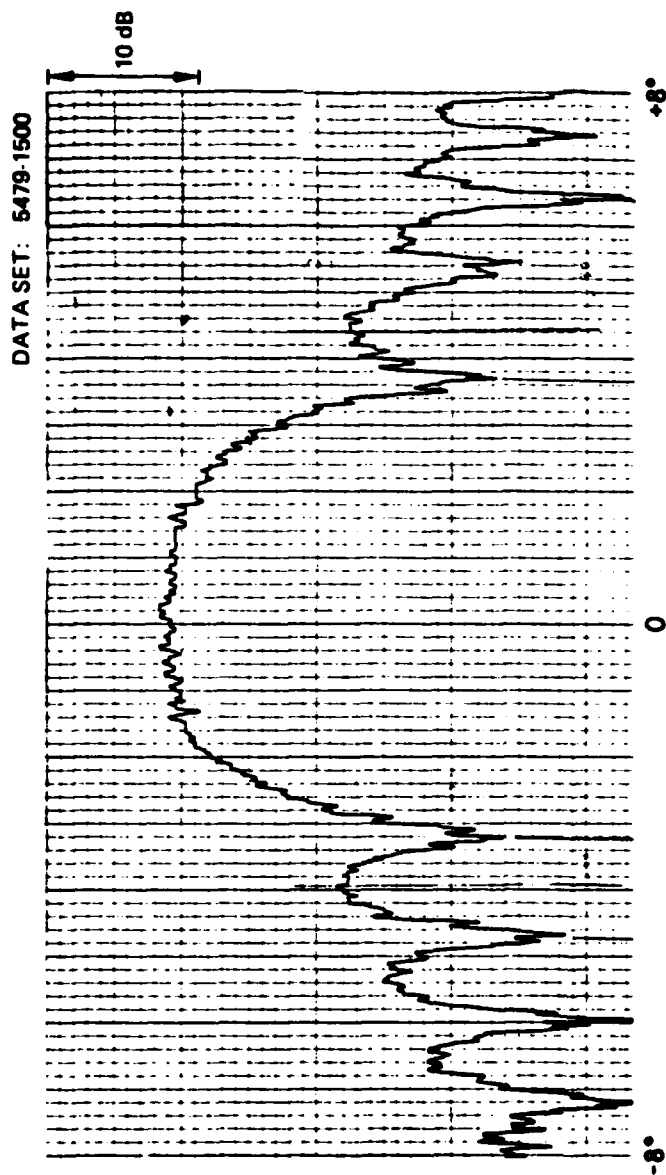


FIGURE 10
PARRAY BEAM PATTERN - STAGE I SEA TEST
 $f = 731 \text{ Hz}$

ARL:UT
AS-80-1799
TGG - GA
11-12-80

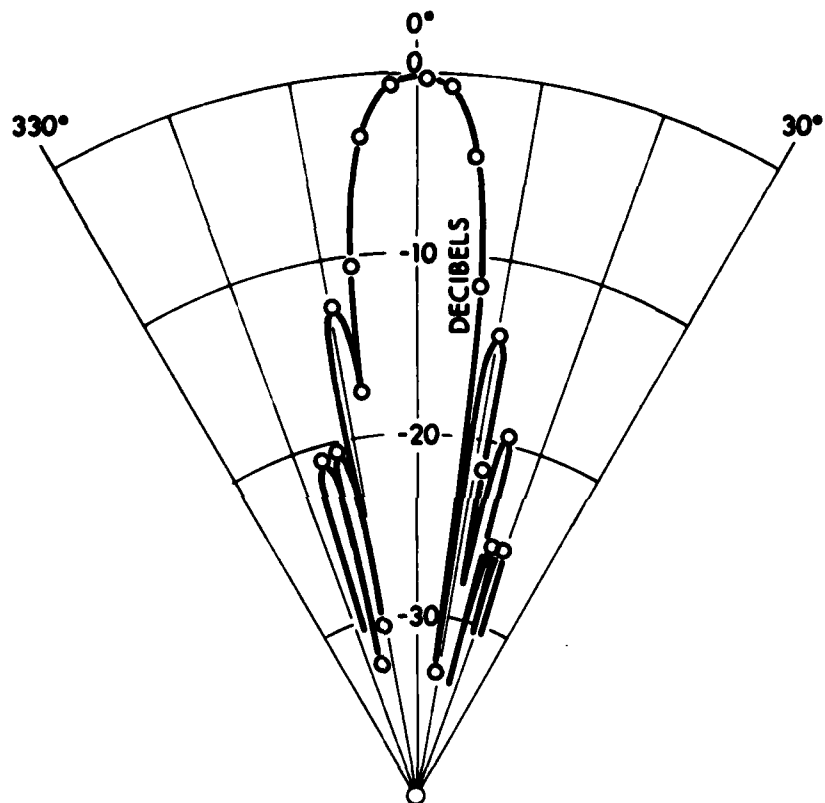


FIGURE 11
PARRAY BEAM PATTERN – STAGE I SEA TEST
 $f = 319 \text{ Hz}$

ARL:UT
 AS-80-1800
 TGG - GA
 11-12-80

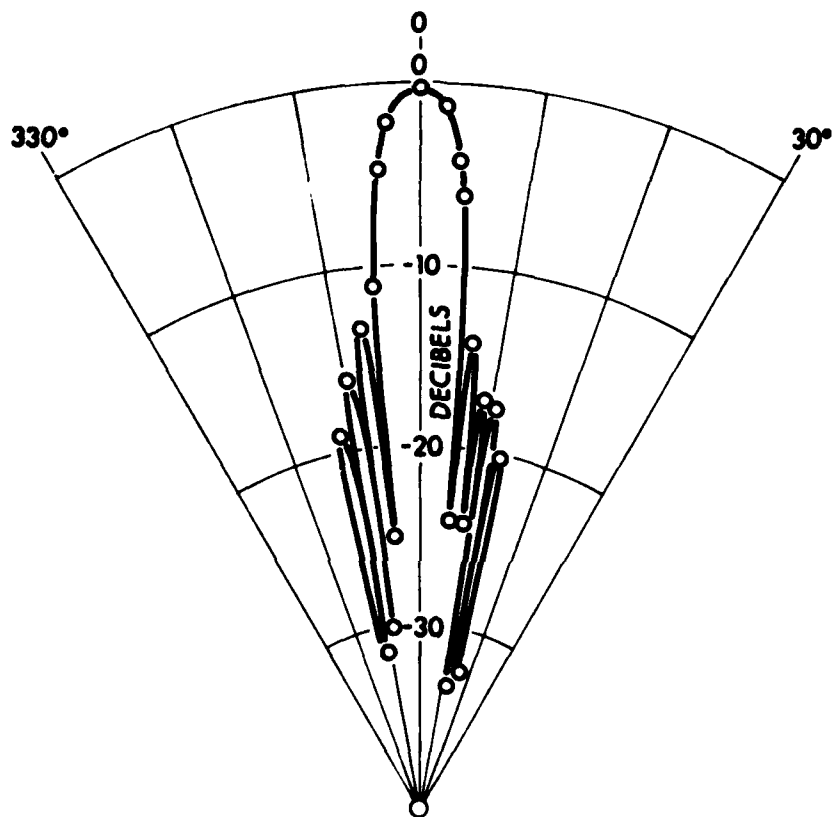
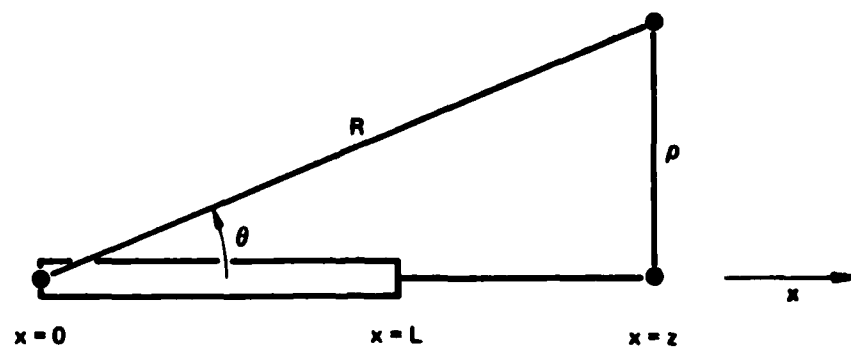
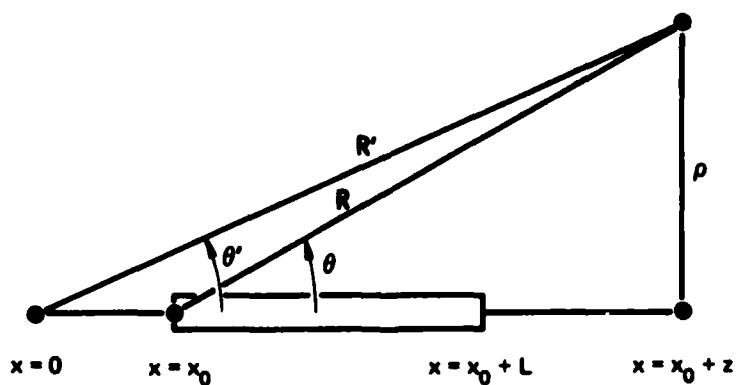


FIGURE 12
PARRAY BEAM PATTERN – STAGE I SEA TEST
 $f = 731 \text{ Hz}$

ARL:UT
 AS-80-1801
 TGG - GA
 11-12-80



(a) THEORETICAL GEOMETRY



(b) EXPERIMENTAL GEOMETRY

FIGURE 13
PARRAY GEOMETRIES FOR STAGE I SEA TEST

ARL:UT
AS-80-1818
TGG - GA
11-12-80

This expression can be evaluated numerically to obtain theoretical beam patterns.

Before comparing theory to experiment, a transformation must be applied to the experimental geometry, shown in Fig. 13(b), so that it corresponds to the theoretical configuration. Experimental measurements of θ' and R' were made from a platform located on the PARRAY axis at a distance $x_0 = 122$ m from the PARRAY hydrophone. Transformation of θ' and R' to θ and R , respectively, may be accomplished as follows:

$$\theta = \tan^{-1} \left[\frac{(x_0 + z) \tan \theta'}{z} \right] , \quad (2)$$

and

$$R = \left[(R')^2 - (x_0^2 + 2x_0 z) \right]^{1/2} , \quad (3)$$

where $z = R' \cos \theta' - x_0$. Measured values are thus compared to predicted values by transforming $D(R', \theta')$ to $D(R, \theta)$ using Eqs. (2) and (3).

3. Comparison of Theoretical Beam Patterns with Measurements

Comparisons of predicted and measured beam patterns are shown in Figs. 14-16. Selected points from the measured patterns were transformed as described above and are shown in the figures by the open dots. Theoretical beam patterns, shown as continuous lines, were obtained using Eq. (1). It can be seen from the figures that the experimental beam patterns are still somewhat narrower than predicted. This may be due to the boundary conditions associated with the measurements; i.e., the beam patterns were taken in shallow water. Specifically, if most of the energy from the low frequency source arrived at the PARRAY at a nonzero elevation angle, then the measured beam pattern would have effectively been in a plane that is tilted to the PARRAY acoustic axis. Such a situation would tend to reduce the width of the measured beam.

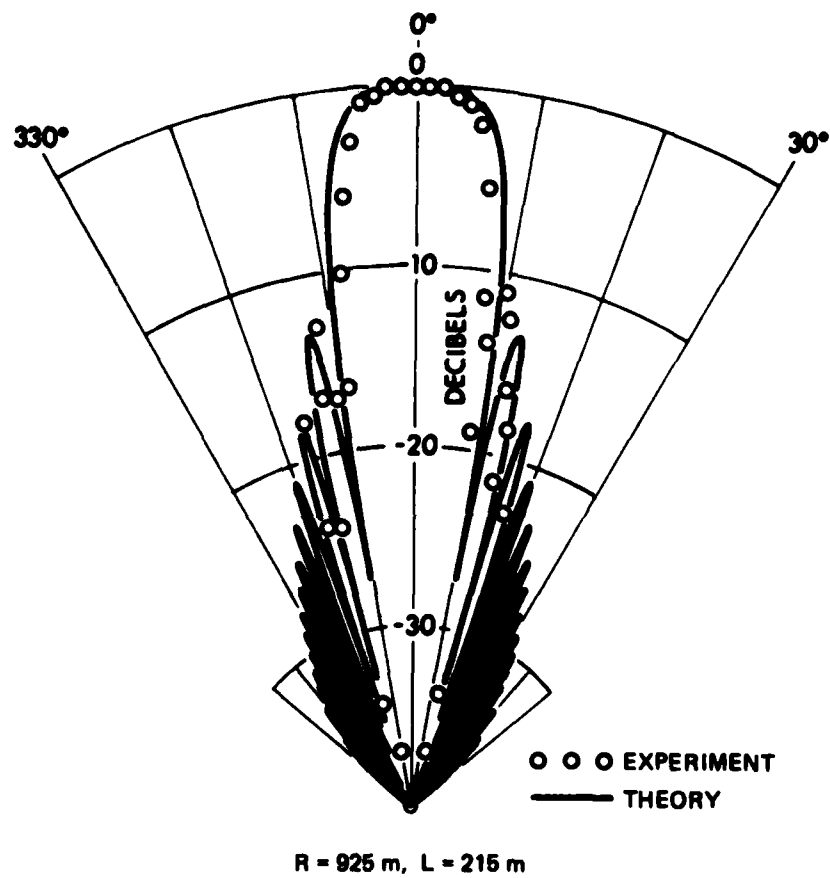


FIGURE 14
PARRAY BEAM PATTERN AT 319 Hz

ARL:UT
AS-80-1802
TGG - GA
11-12-80

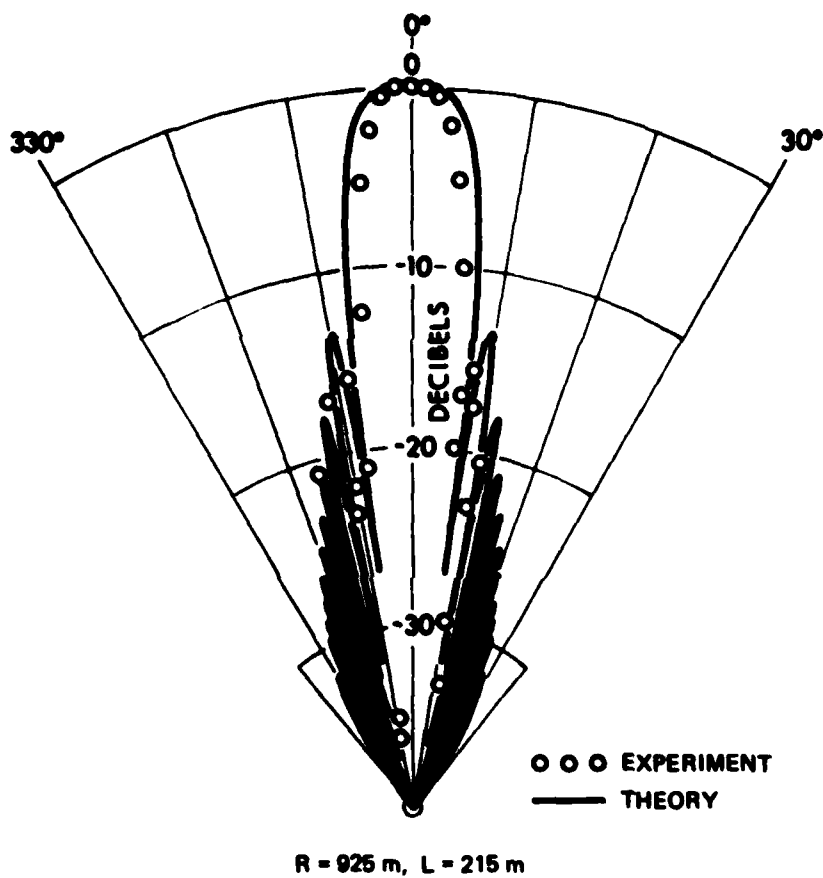


FIGURE 15
PARRAY BEAM PATTERN AT 543 Hz

ARL:UT
AS-80-1803
TGG - GA
11-12-80

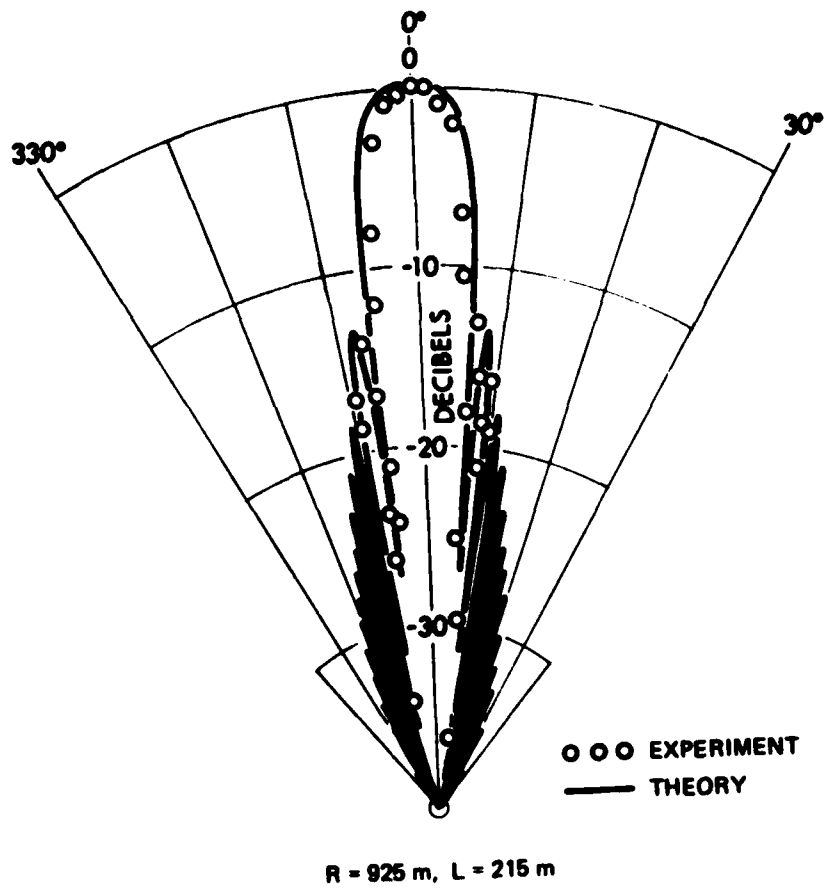


FIGURE 16
PARRAY BEAM PATTERN AT 731 Hz

ARL:UT
AS-80-1804
TGG - GA
11-12-80

C. Ambient Noise

The ambient noise near Stage I was measured over a wide range of frequencies using several sensors: an H23 standard hydrophone located near the edge of the stage, an F50 standard hydrophone at each of the PARRAY towers, and the planar array used as the PARRAY hydrophone. In general, the amplitude of noise in shallow water is much higher than that in the deep ocean. Since the noise measurements were all made within 350 m of Stage I, additional noise sources were present. The noise created by waves slapping the Stage I support structure, generator noise from the Stage I power sources, and biologic noise from the marine life attracted to the platform added to that of the normal shallow water levels. Although the parametric receiver was oriented in a direction to reject much of the Stage I noise, the dominant noise source, especially at the higher frequencies, was snapping shrimp. The latter noise was characterized by short duration high level impulses of sound, concentrated in the immediate vicinity of Stage I, and tapering off away from the platform.

Noise levels for a fairly calm sea (SS1) were measured using the H23 standard hydrophone at a depth of 10 m near the edge of Stage I. The measurement was made using a swept filter analyzer with a bandwidth of 300 Hz. The measured levels were reduced to an equivalent 1 Hz spectrum level and are shown in Fig. 17. The data cover a frequency range from 1 to 50 kHz.

The ambient noise level near 65 kHz was measured using the PARRAY hydrophone, which had a half-power beamwidth of 5.6° and a directivity index of 30 dB. The noise at the pump frequency was dominated by the snapping shrimp and indicated little correlation with time of day or sea state. The spectrum level, shown in Fig. 8, was about 53 dB re $1 \mu\text{Pa}/\sqrt{\text{Hz}}$. This level restricted some measurements of PARRAY operation, but was not high enough to affect the basic tests for system validation.

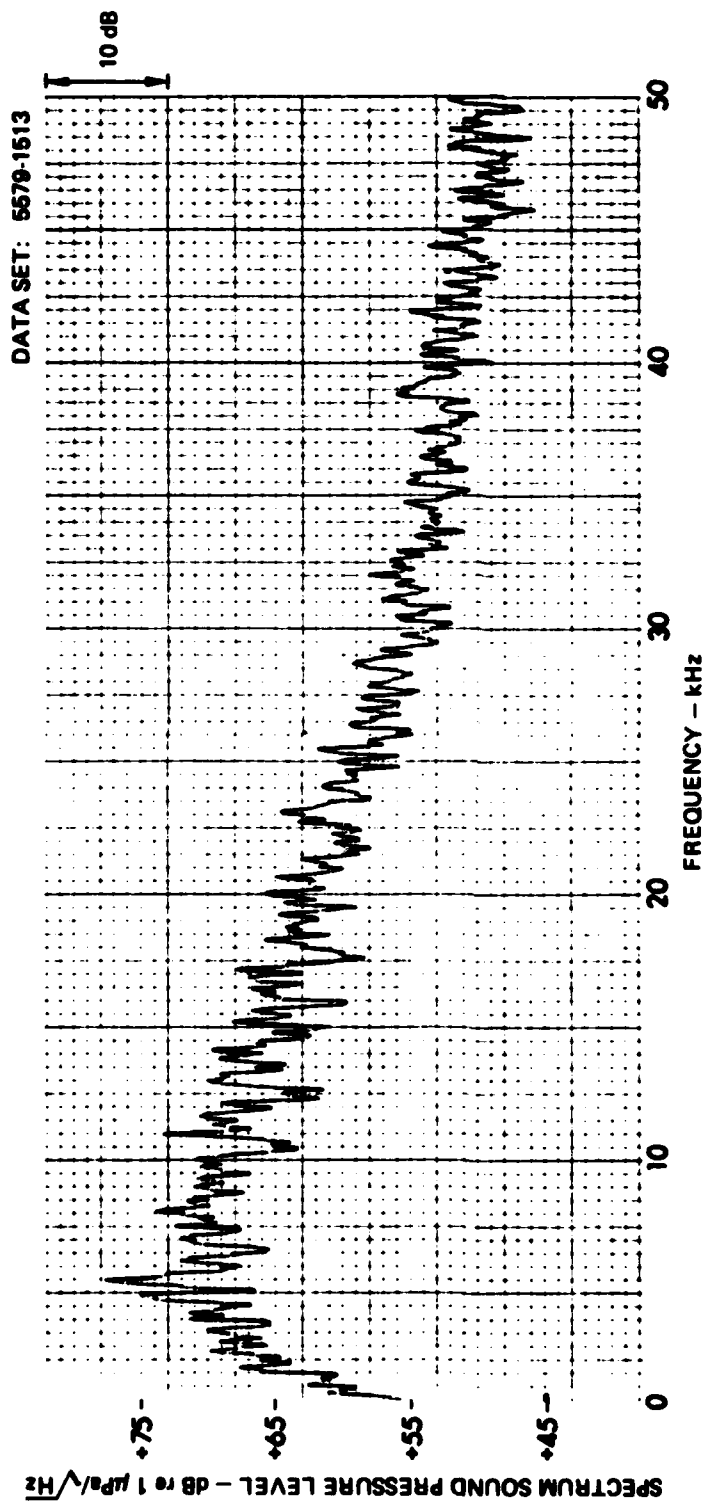


FIGURE 17
 AMBIENT NOISE AT STAGE I DURING PARRAY SEA TEST
 H23 HYDROPHONE

ARL:UT
 AS-80-1806
 TGG - GA
 11-12-80

Ambient noise in the low audio frequency range was measured using the F50 hydrophones on the PARRAY underwater towers. The curve of Fig. 18 labeled F50 shows background noise level at the hydrophone tripod, approximately 2 m off the bottom. The level varied by as much as 10 dB with changes in sea state. The large peaks at 180, 240, and 360 Hz are related to the power sources on the Stage I platform.

The two lower curves in Fig. 18 are reproduced from Fig. 8. They show that the output of the PARRAY was not limited by spectral purity of the pump signal or by electronic noise in the receiver electronics for these tests.

D. Array Gain Measurements

The array gain of the PARRAY was measured under various weather and operational conditions. A comparison between the upper sideband (USB) signal from the PARRAY and the signal from the F50 is shown in Fig. 18. The PARRAY USB output indicates an array gain of approximately 20 dB at a frequency of 400 Hz. The gain does not increase substantially at higher frequencies because of contributions from the ambient acoustic noise near the pump frequency. Since the low frequency ambient noise is reduced by the spatial processing gain of the PARRAY, additional gain would be realizable for a more moderate pump ambient noise condition at the pump sideband frequency. If the level of high frequency noise was due only to sea state, the PARRAY could provide an additional 6-10 dB of array gain. The limiting case then would be the sideband noise from the pump electronics, and receiver electronic noise. For this unusually high noise condition the MDL is not representative, but for moderate shallow water conditions an MDL of 35 dB re $1 \mu\text{Pa}/\sqrt{\text{Hz}}$ should be feasible.

E. Signal Stability

The acoustic signals received by the PARRAY must have sufficient phase stability to permit narrowband processing without significant spectral spreading. Since the PARRAY uses the medium for beam formation,

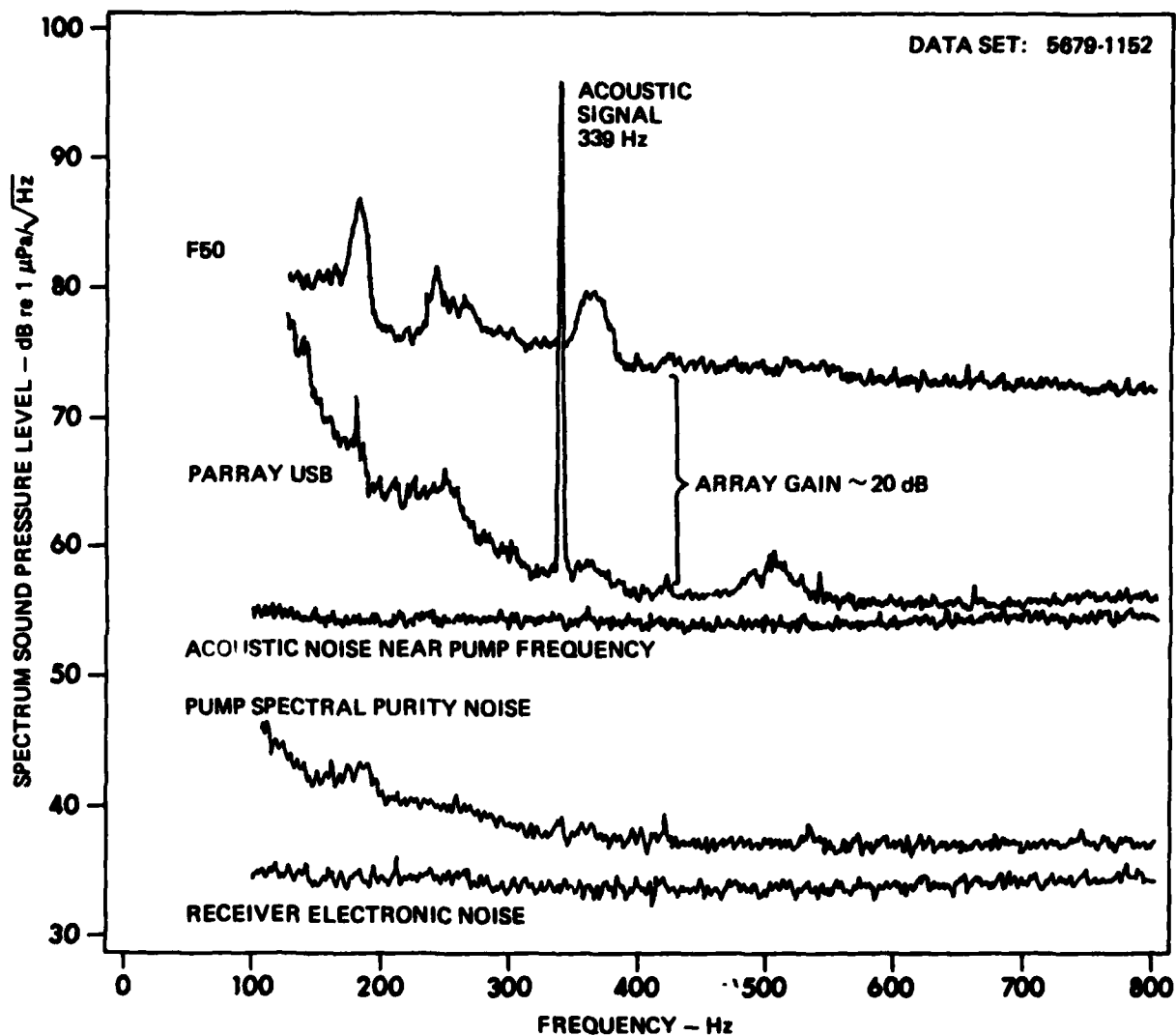


FIGURE 18
COMPARISON OF PARRAY OUTPUT WITH REFERENCE HYDROPHONE OUTPUT
AND PUMP FREQUENCY ACOUSTIC AMBIENT NOISE AT STAGE I

ARL:UT
 AS-80-1808
 TGG - GA
 11-12-80

the phasing process should not vary sufficiently to alter the signal stability. A J15 transducer was mounted approximately 1 m off the bottom at a range of approximately 700 m from the PARRAY hydrophone. A stable signal at a frequency of 329 Hz was transmitted by the J15. The upper sideband output from the PARRAY receiver was analyzed with 0.01 Hz resolution. The data in Fig. 19 show that there was no appreciable spectral spreading of the signal received by the PARRAY.

F. Effects of Thermal Gradients on Propagation

Propagation of signals in the shallow water environment near Stage I was a complex process. An effort was made to perform the sea test at a time of year that would minimize the effects of thermal gradients. The 30 m water depth at Stage I is much shallower than that contemplated for any realistic application of the PARRAY, but the Stage I location did provide an accessible and low cost test site. Thermal gradients did, however, have an effect on the experiments, especially in the latter stages of the tests. In particular, propagation of the pump beam and of the low frequency signals were affected by thermal gradients.

The narrowbeam pump signal was transmitted approximately 5 m above the bottom to the PARRAY hydrophone at a range of 215 m. The pump carrier signal received at the hydrophone remained quite stable throughout most of the tests; however, on the last day of the sea test the temperature gradient was severe enough to cause some deflection of the pump beam. This in turn resulted in a reduced carrier level as well as a measurable amount of amplitude fluctuation (~5%), even after realignment of the planar arrays. Thus, it may be concluded that a significant reduction in performance can be expected wherever a PARRAY is required to operate in shallow water near a thermal layer.

The effects of differing sound velocity profiles on the propagation of signals near Stage I are illustrated in Figs. 20, 21, and 22 for three different sound speed profiles, denoted conditions A, B,

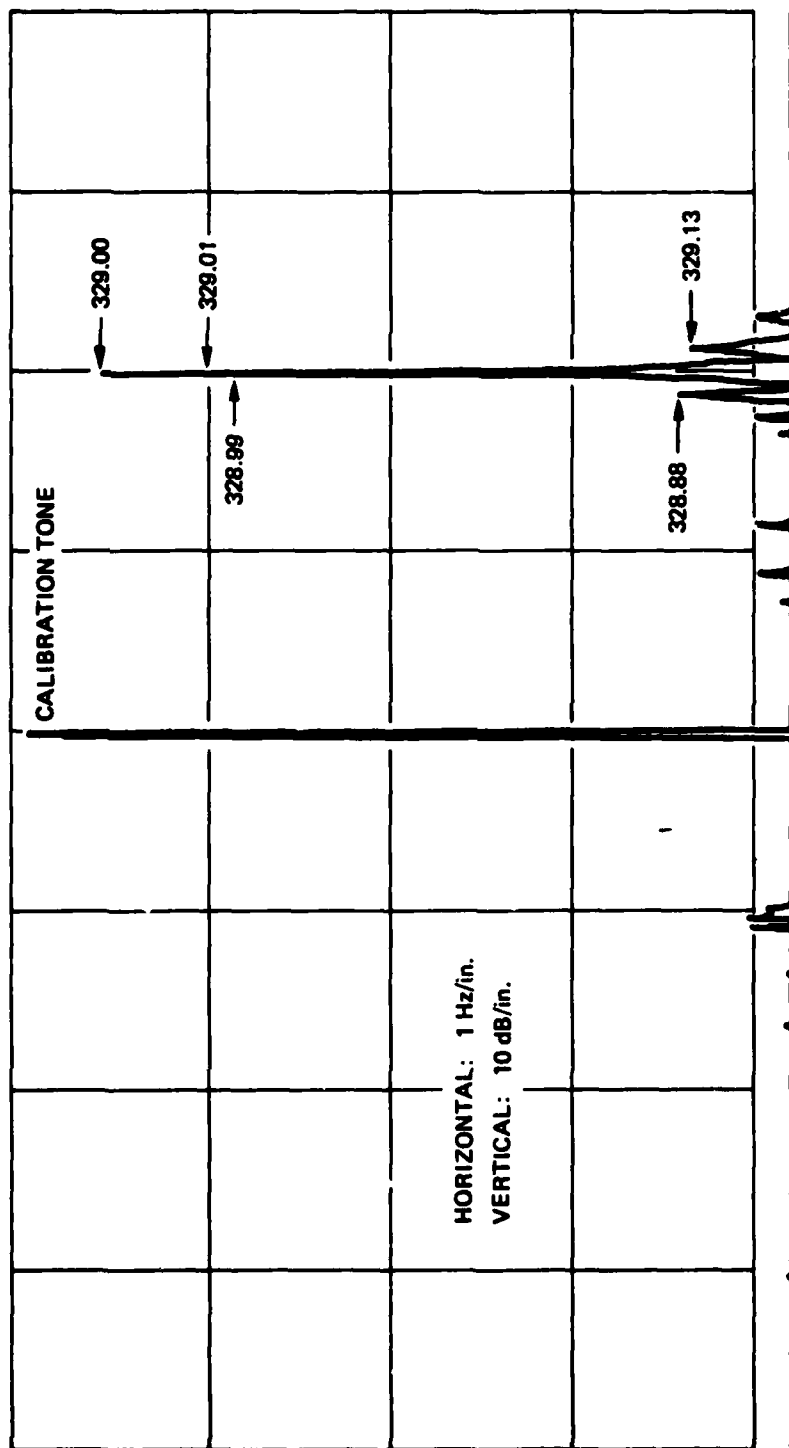


FIGURE 19
PARRAY SIGNAL STABILITY TEST RESULTS
NARROWBAND PROCESSING 0.01 Hz BANDWIDTH
 $f_s = 329 \text{ Hz}$

ARL:UT
AS-80-1808
TGG - GA
11-12-80

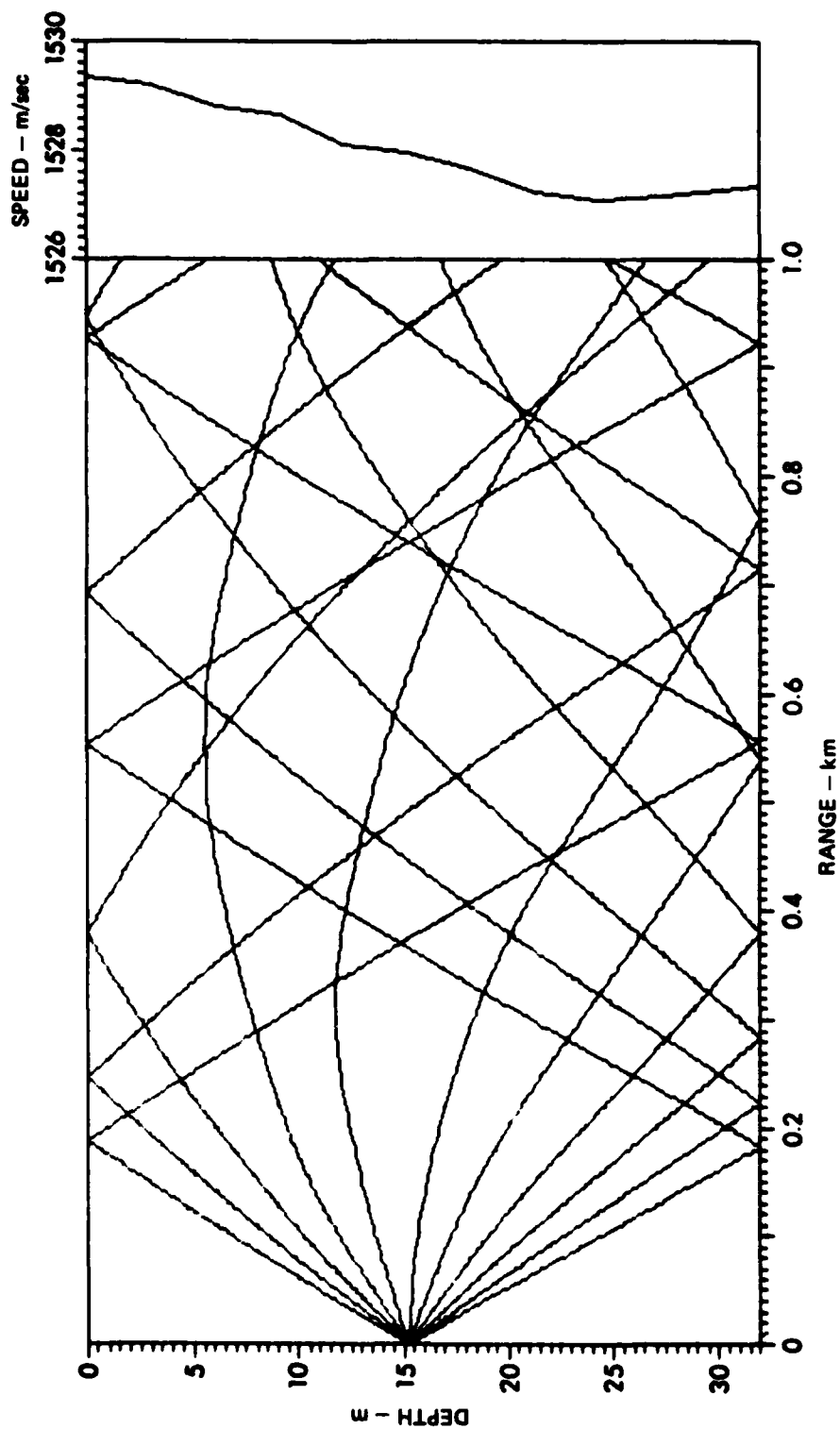


FIGURE 20
RAYPATH PLOT FOR J13 SOURCE AT MIDDEPTH - SOUND SPEED PROFILE A

ARL:UT
AS-80-1808
TGG - GA
11-12-80

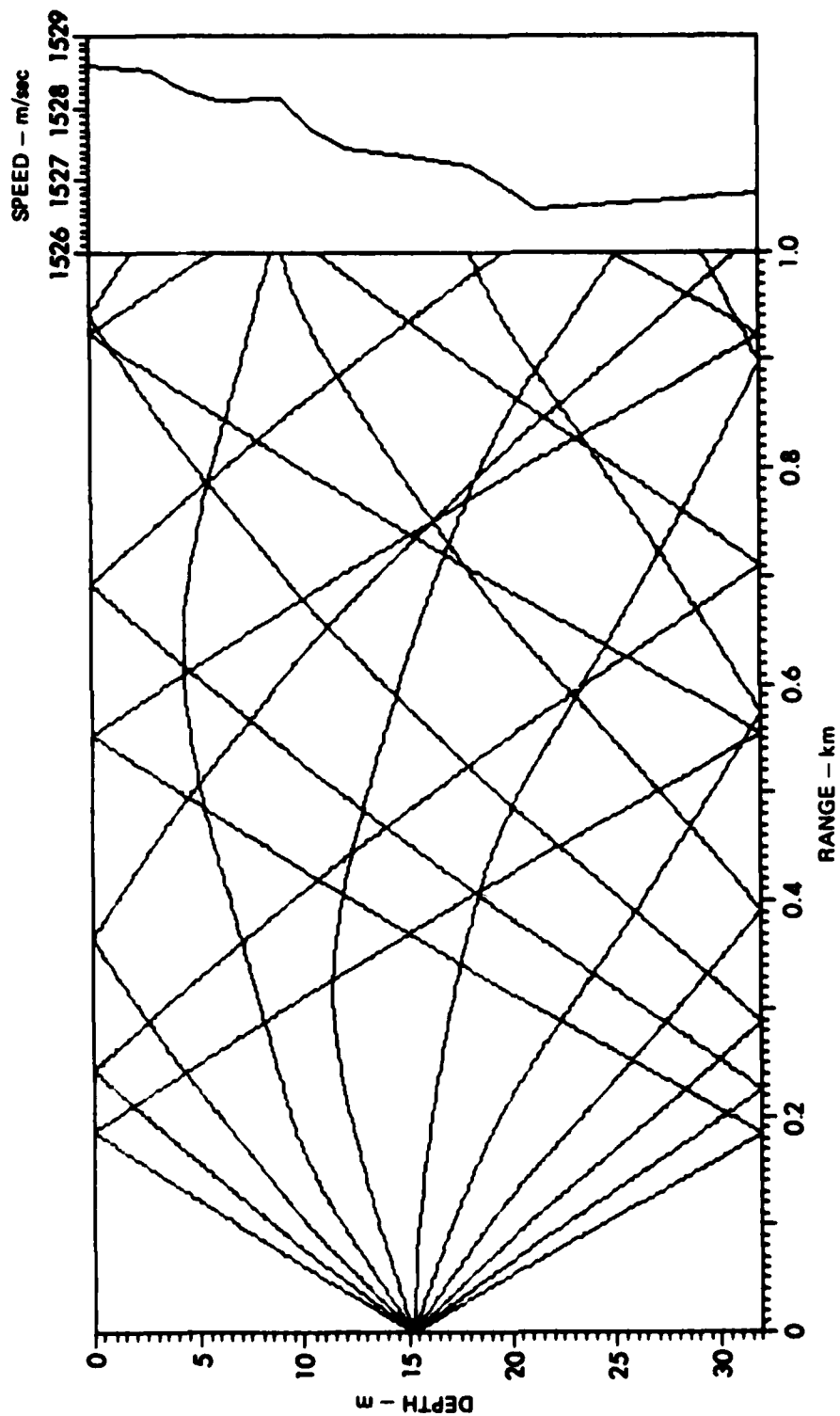


FIGURE 21
RAYPATH PLOT FOR J13 SOURCE AT MIDDEPTH - SOUND SPEED PROFILE B

ARL:UT
AS-80-1810
TGG - GA
11-12-80

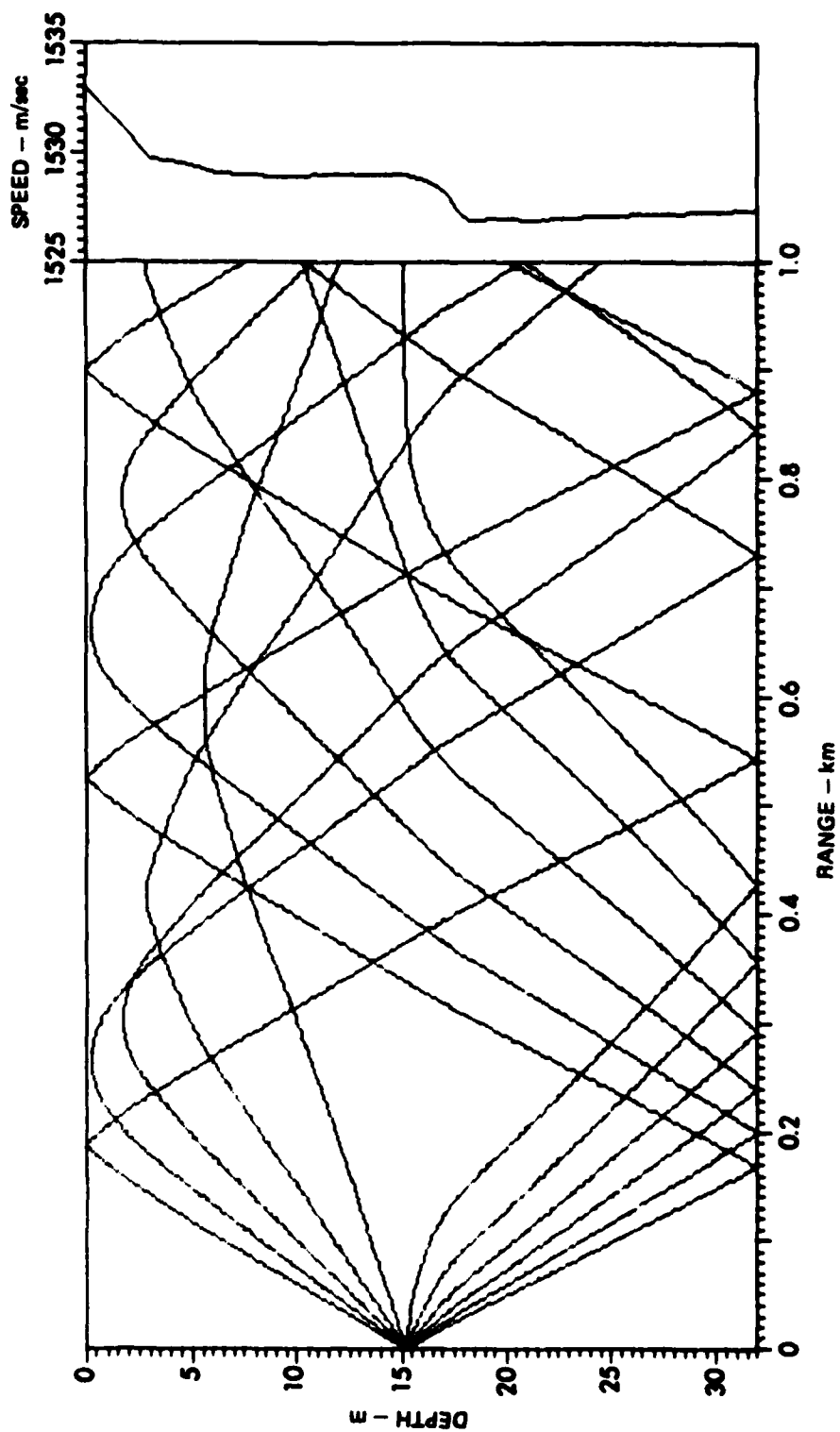


FIGURE 22
RAYPATH PLOT FOR J13 SOURCE AT MIDDEPTH - SOUND SPEED PROFILE C

ARL:UT
AS-60-1811
TGG - GA
11-12-80

and C, respectively. The raypath plots in each case cover the sector $\pm 5^\circ$ about the horizontal in 1° increments for the source at a depth of 15 m. The sound speed profiles are representative of those observed during the sea test. The layer at the deeper depths became more pronounced toward the end of the sea test and propagation conditions changed noticeably. For the conditions of Fig. 22, it can be seen that no direct path extends farther than 500 m. For tests performed with a source greater than 500 m in range, the only arrival is from a surface reflection or other multiple reflected paths such as surface-bottom, bottom-surface, surface-bottom-surface, etc.

Tests were also performed with the NRL/USRD J15 transducer mounted approximately 2 m off the bottom; the effects of changes in sound speed on propagation are shown in Figs. 23, 24, and 25. It may be seen that the sound had to arrive at the PARRAY from a range of 500-700 m through multiple bounce paths.

G. Effects of Shallow Water on Parametric Reception

1. Introduction

If a water column is sufficiently shallow, sound propagation will be greatly affected by the surface and bottom boundaries. In general, the pressure field observed in shallow water will depend upon the depth of both the source and the receiver, and upon the sound velocity profile in the water column. There are two theoretical methods for calculating the pressure field in shallow water: ray theory and normal mode theory. Ray theory represents the sound field as a sum of ray contributions emanating from the source and its various images in the surface and bottom. Normal mode theory expresses the sound field as the sum of modes, each mode being a complicated function representing a wave radiated from the source with an amplitude that is dependent on source and receiver depths. Ray theory is most useful at short ranges, where few images are required in approximating the sound field. At long ranges, where only a few modes are required to describe the transmission, normal

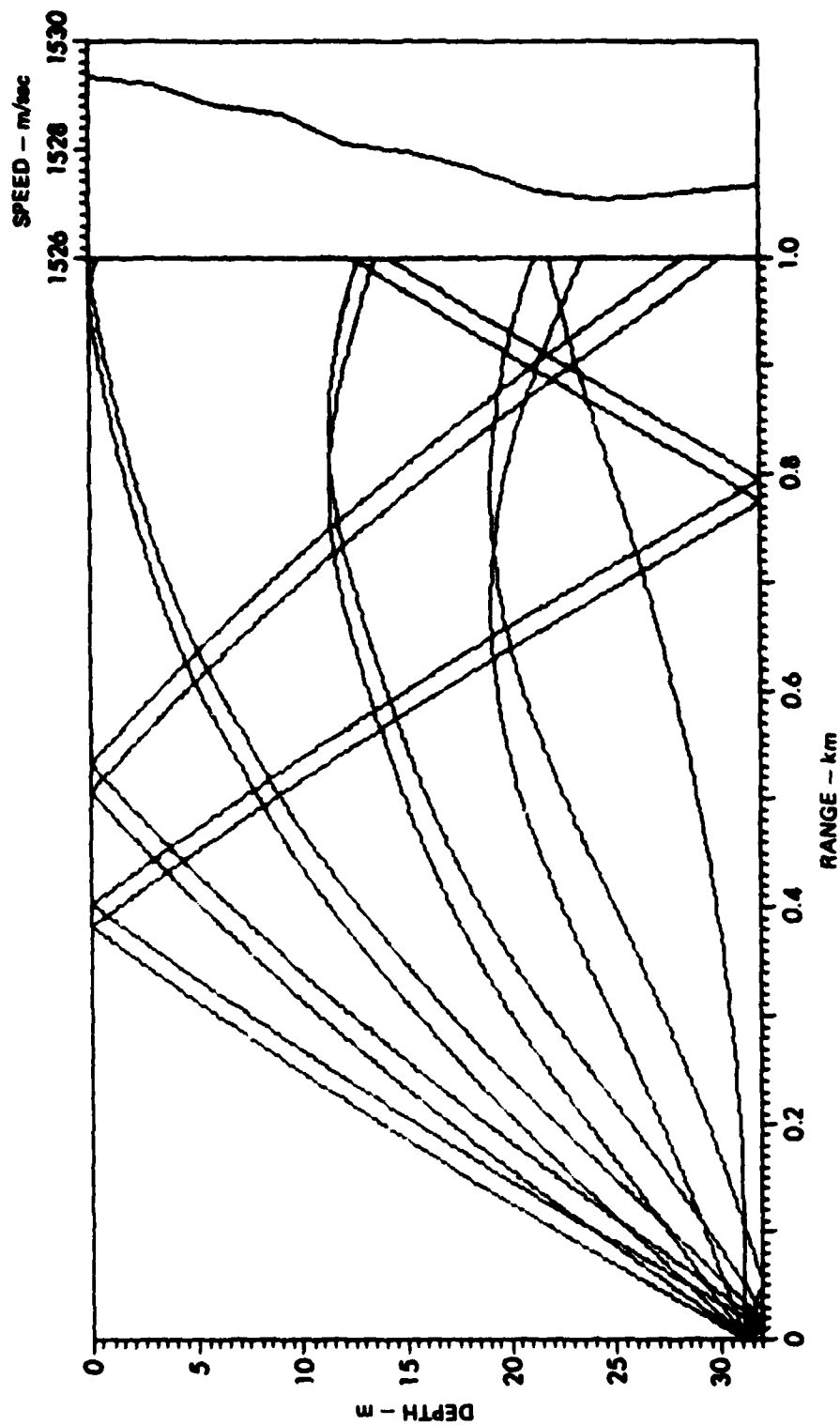


FIGURE 23
RAYPATH PLOT FOR J15 SOURCE NEAR BOTTOM - SOUND SPEED PROFILE A

ARL:UT
AS-80-1812
TGG - GA
11-12-80

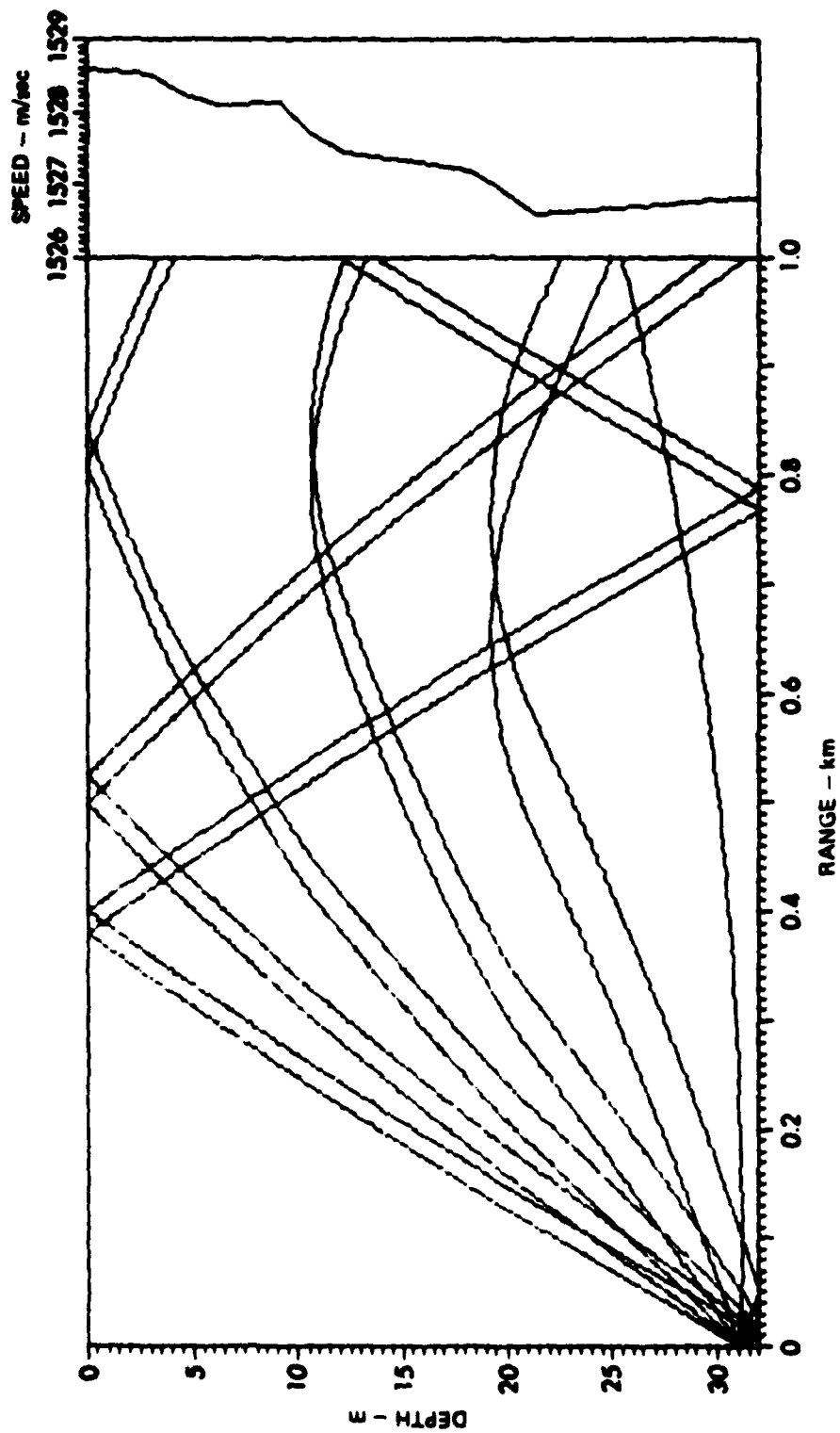


FIGURE 24
RAYPATH PLOT FOR J15 SOURCE NEAR BOTTOM - SOUND SPEED PROFILE B

ARL:UT
AS-80-1813
TGG:GA
11-12-80

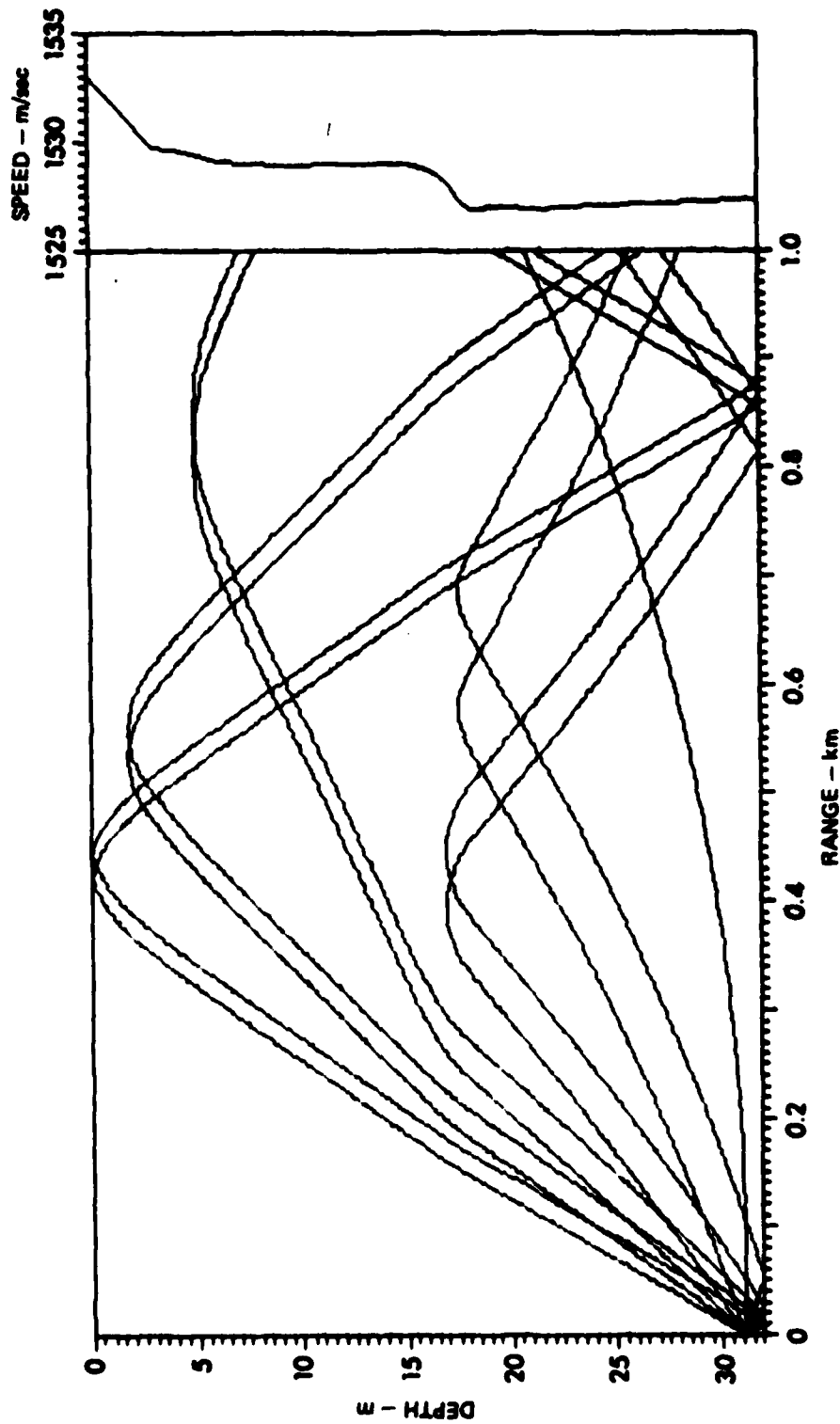


FIGURE 25
RAYPATH PLOT FOR J15 SOURCE NEAR BOTTOM - SOUND SPEED PROFILE C

ARL:UT
AS-80-1814
TGG - GA
11-12-80

mode theory is more useful. A "crossover" range demarcating the regions of usefulness of the two theories is given by⁸

$$r_o = \frac{H^2}{\lambda} \quad , \quad (4)$$

where

H = water depth, and

λ = wavelength.

For the experiments at Stage I, where H = 30 m, r_o is shown as a function of frequency in Fig. 26. Because the ranges used in most of the experiments at Stage I exceeded the crossover range r_o , normal mode theory is required to describe the low frequency pressure waves as they propagate from signal source to the PARRAY interaction volume. Although a complete theory has not yet been developed for the effects of shallow water on parametric reception, significant features of these effects can be determined by considering some basic results of normal mode theory.

2. Application of Normal Mode Theory to a Directional Receiver in Shallow Water

As discussed above, a sound field in shallow water can be represented as a sum of normal modes. Each mode corresponds to a pair of plane waves propagating in a zigzag fashion through the sound channel, each wave being incident upon the surface or bottom at a grazing angle β . If the sound channel can be modeled as a pressure-release surface and a rigid bottom, then the mode grazing angle β associated with mode number n is given by⁸ assuming a bottom mounted source,

$$\beta = \sin^{-1} \left[\left(n - \frac{1}{2} \right) \frac{\lambda}{H} \right] \quad . \quad (5)$$

When a directional receiver is placed in the sound channel, as shown schematically in Fig. 27, only those modes with grazing angles less than the half-power angle $\theta_{1/2}$ of the receiver will contribute significantly to the received sound level. Modes with grazing angles greater

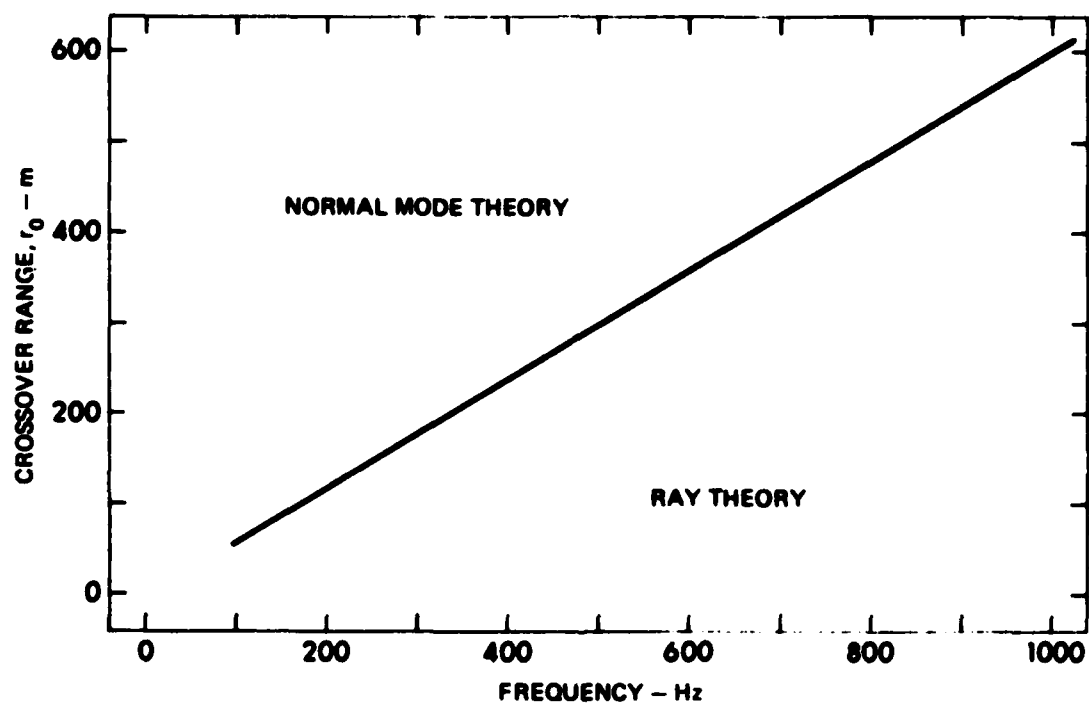


FIGURE 28
CROSSOVER RANGES FOR LOW FREQUENCY
PROPAGATION MODELS IN 30 m DEEP WATER

ARL:UT
AS-80-1815
TGG - GA
11-12-80

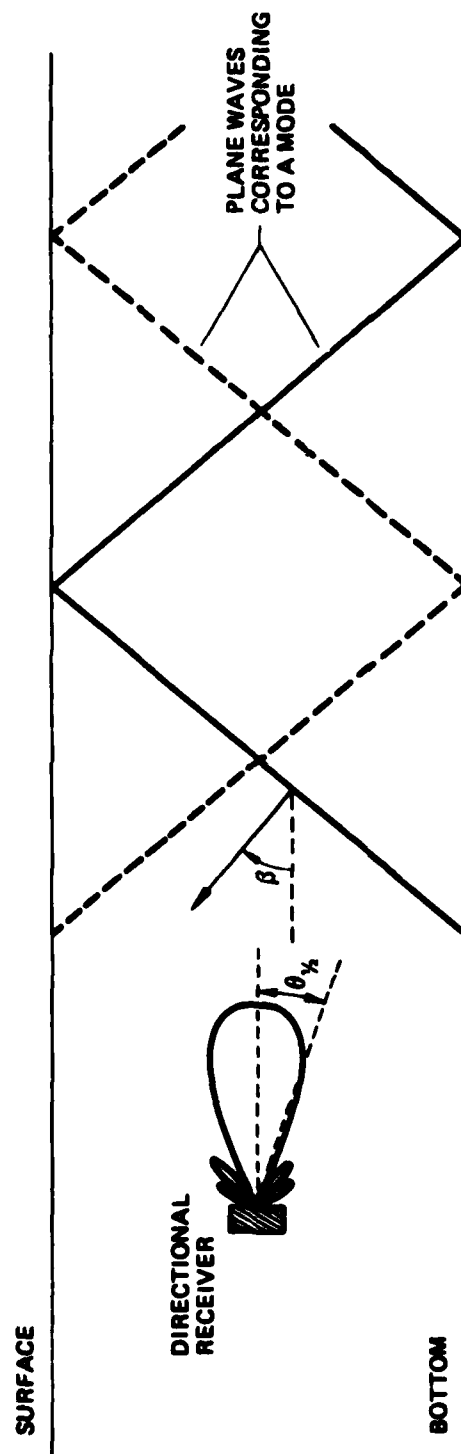


FIGURE 27
DIRECTIONAL RECEIVER IN SHALLOW WATER

ARL:UT
AS-60-1816
TGG-GA
11-12-80

than $\theta_{1/2}$ will be attenuated by the directivity of the receiver. Because a directional receiver will attenuate modes having sufficiently large grazing angles, it will not sense the complete sound field. One consequence of this is that, given the same source level and range, the voltage output of a directional receiver in shallow water will be less than the corresponding output of an omnidirectional receiver. In other words, there is a loss in detected intensity associated with directional reception in shallow water.

By treating the PARRAY as a directional receiver, these simple considerations can be extended to parametric reception. Therefore, the PARRAY may be expected to discriminate against modes having values of β that are greater than the half-power angle of the PARRAY. As a result, the level of the sideband pressure detected by the PARRAY in shallow water will, for a given signal source level and sufficiently large values of β , be less than the corresponding level of the pressure detected by an omnidirectional receiver.

3. Effects of Shallow Water on the Experimental PARRAY at Stage I

To evaluate the effects of shallow water on the performance of the PARRAY at Stage I, a comparison will be made between the response of the PARRAY and that of an omnidirectional hydrophone for identical transmissions.

The sound pressure level (SPL) of a low frequency transmitted signal, measured at the hydrophone of the PARRAY, will be given by⁸

$$SPL_T = SL - TL \quad , \quad (6)$$

where

SL = the source level in dB re 1 μ Pa at 1 m,

TL \pm 20 log r + α r + 60 - k_L dB,

r = range in kilometers,

α = attenuation coefficient in dB/km, and

k_L = nearfield anomaly.

The parameter k_L is tabulated in Ref. 8. For the present experiment, $k_L \approx 6$ dB.

Table II compares typical values of SPL measured with the PARRAY (SPL_p), measured with an omnidirectional sensor placed near the PARRAY hydrophone (SPL_o), and computed using Eq. (6) (SPL_T). The values of SPL_p and SPL_o were obtained simultaneously on 2 May 1979 at 1525 h with a southeasterly wind of approximately 14-15 kt and wave heights of 0.6 to 1 m. It can be seen from Table II that, with the exception of the 561 Hz signal, there is reasonably good agreement between the levels measured by the omnidirectional hydrophone and those predicted by Eq. (6). It can also be seen that the levels measured by the PARRAY are consistently lower than those predicted by theory. This loss in level can be explained by employing the considerations developed in the previous section.

For the experiments at Stage I, the PARRAY can be modeled as a directional receiver with half-power angle (in degrees) given by

$$\theta_{1/2} = 52.5 \sqrt{\lambda/L} \quad . \quad (7)$$

A comparison is made in Fig. 28 between $\theta_{1/2}$ for the PARRAY and grazing angle β for modes 1, 2, and 3, where β is given by Eq. (4). It can be seen that, for frequencies less than 800 Hz, only the grazing angles of the first mode are less than corresponding values of $\theta_{1/2}$. This means that only the first mode can be expected to contribute significantly to the sound level measured by the PARRAY for frequencies less than about 800 Hz. Since the maximum effective source level for any single mode is approximately 20 dB below the freefield source level,⁹ it may be expected that a PARRAY receiving only the first mode would show a response approximately 20 dB below freefield response.

In light of these considerations, the results in Table II seem quite reasonable. SPL_p is consistently less than SPL_o or SPL_T , with the magnitude of the difference varying from 6 to 28 dB. There are two

TABLE II
COMPARISON OF MEASURED AND THEORETICAL
SOUND PRESSURE LEVEL (SPL)

FREQUENCY Hz	SPL _O dB re 1 μ Pa	SPL _P dB re 1 μ Pa	SPL _T dB re 1 μ Pa
137	98	91	97
311	92	86	93
561	79	62	90
753	85	72	88

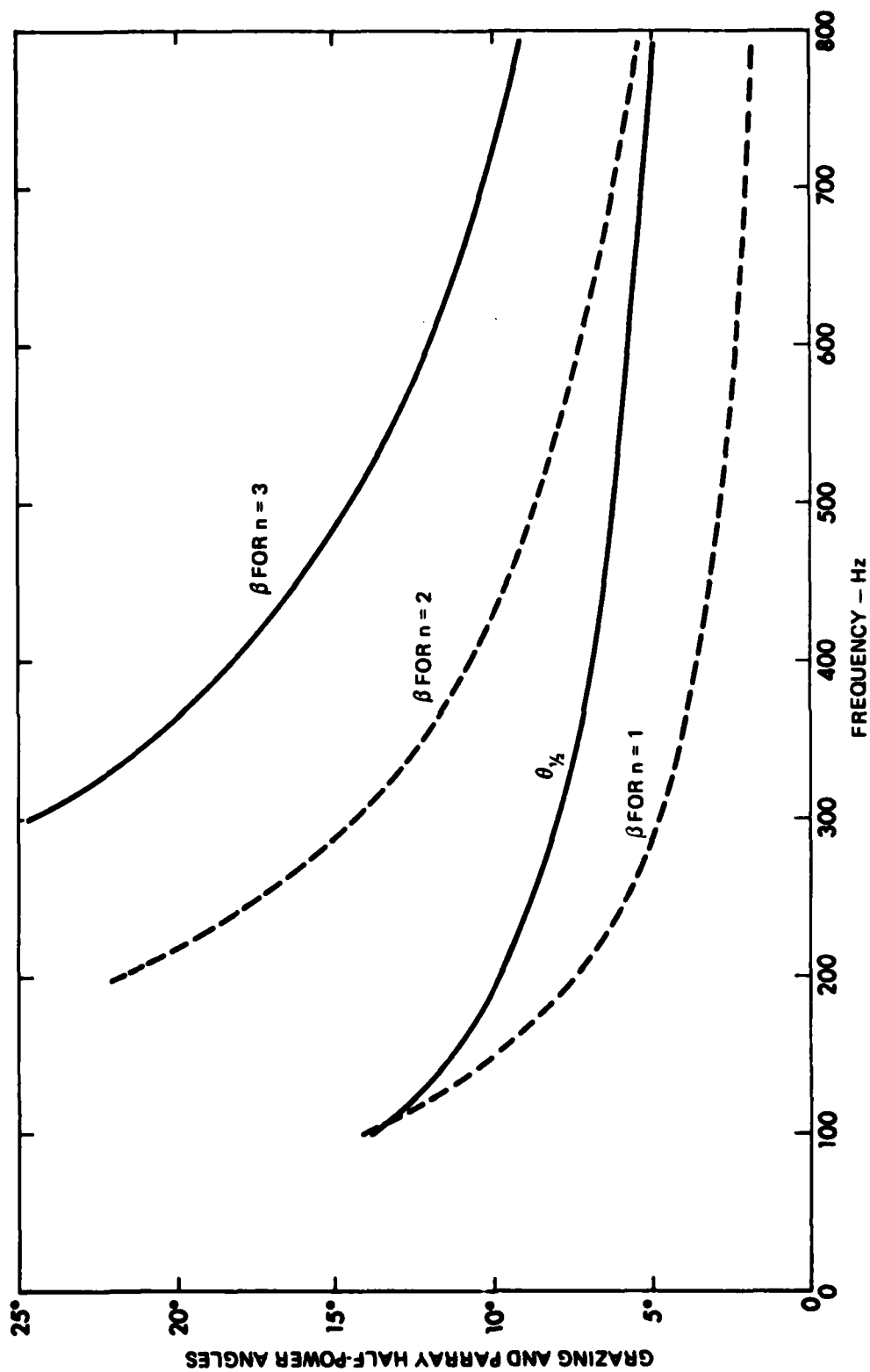


FIGURE 28
COMPARISON OF PARRY HALF-POWER ANGLE AND GRAZING ANGLE

ARL:UT
AS-60-1817
TGG-GA
11-12-80

reasons why SPL_p may be expected to vary with signal frequency. One is that the pressure amplitude of each mode is frequency dependent so that, if the PARRAY is receiving only the first mode, its response may be expected to vary with frequency. Another reason is that the mode grazing angles as well as the PARRAY beamwidth change with frequency, so that the level of higher order modes measured by the PARRAY is frequency dependent.

4. Conclusions Regarding Effects of Shallow Water

It has been shown qualitatively that a PARRAY operating in shallow water may be expected to detect only those modes which have grazing angles less than the half-power angle of the PARRAY. Consequently, the response of the PARRAY to a low frequency signal in shallow water may be expected to be less than the corresponding response of an omnidirectional sensor. This expectation of reduced response in shallow water was confirmed by the experimental results obtained at Stage I.

In comparing the responses of directional and omnidirectional receivers in shallow water, however, it should be noted that although the signal level detected by the directional sensor may be less, the ambient noise detected by the directional receiver will also be less. Thus it is still possible to obtain a S/N improvement compared to an omnidirectional receiver by employing a directional receiver in shallow water.

A detailed theoretical and experimental study of the effects of shallow water on parametric reception was beyond the scope of the task described here. Such a study would be a worthwhile task because it would shed light on the complicated problem of nonlinear acoustic interaction in a bounded medium, and also give useful insights on directional reception in shallow water.

V. SUMMARY AND CONCLUSIONS

Applied Research Laboratories, The University of Texas at Austin, has been engaged in the design, development, and testing of an experimental, large aperture parametric acoustic receiving array (PARRAY). The experimental PARRAY was installed and tested in 30 m deep water in the Gulf of Mexico at the Stage I facility of Naval Coastal Systems Center. The pump and hydrophone were installed 5 m above the bottom on tripods 215 m apart.

A number of tests were performed on the experimental PARRAY. Results of these tests demonstrated that a directional receiving array with processing gain was formed. These tests also confirmed previously developed systems' models of the effects of various contributors to the self-noise floor of the PARRAY. The tests at Stage I were a logical extension and validation in the ocean environment of the results of earlier tests in Lake Travis, Texas.² The dominant contributor to the noise floor of the PARRAY at Stage I was found to be marine life in general and snapping shrimp in particular.

Some anomalous results were obtained in measured beam patterns and in signal levels received with the experimental PARRAY. Subsequent analysis showed that these results were to be expected in very shallow water and with the relatively short ranges used in the experiments.

In conclusion, the objectives of the PARRAY sea test, to determine system minimum detectable level, verify the system model, and determine the effects of the medium and environment on system performance, were achieved on schedule and within the funds allotted. It was demonstrated that the PARRAY is a viable candidate as a sensor for naval application inasmuch as a directional receiving beam was formed in the ocean using

only two transducers and some associated electronics. The behavior of the PARRAY in a shallow water environment was identified as an area for future research.

REFERENCES

1. Tommy G. Goldsberry, Wiley S. Olsen, C. Richard Reeves, David F. Rohde, and M. Ward Widener, "Investigation of the Parametric Acoustic Receiving Array (PARRAY)" (U), Applied Research Laboratories Technical Report No. 76-36 (ARL-TR-76-36), Applied Research Laboratories, The University of Texas at Austin, 31 December 1976. CONFIDENTIAL (Final Report under Contract N00039-75-C-0207).
2. Tommy G. Goldsberry et al., "Development and Evaluation of an Experimental Parametric Acoustic Receiving Array (PARRAY)," Applied Research Laboratories Technical Report No. 79-5 (ARL-TR-79-5), Applied Research Laboratories, The University of Texas at Austin, 16 February 1979. (Final Report under Contract N00039-76-C-0231.)
3. C. R. Reeves and T. G. Goldsberry, "Test Plan for Interim Lake Tests of the Parametric Acoustic Receiving Array (PARRAY)," Applied Research Laboratories Technical Memorandum No. 77-21 (ARL-TM-77-21), Applied Research Laboratories, The University of Texas at Austin, 23 February 1977.
4. Tommy G. Goldsberry et al., "Parametric Acoustic Receiving Array (PARRAY) Research and Experiments," Applied Research Laboratories Technical Report No. 80-7 (ARL-TR-80-7), Applied Research Laboratories, The University of Texas at Austin, 6 February 1980. (Final Report under Contract N00039-78-C-0121.)
5. David F. Rohde, C. Richard Reeves, Tommy G. Goldsberry, and Robert A. Lamb, "Plan for the Sea Test of the Parametric Acoustic Receiving Array (PARRAY)," (U), Applied Research Laboratories Informal Technical Memorandum No. 79-5 (ARL-ITM-79-5), Applied Research Laboratories, The University of Texas at Austin, 27 March 1979.
6. G. G. Salsman and A. J. Ciesluk, "A Description of Environmental Conditions in Coastal Waters Near Panama City, Florida," NCSC Working Paper SP-78-4-056, Naval Coastal Systems Center, Panama City, Florida, November 1977.
7. H. O. Berktaay and J. A. Shooter, "Nearfield Effects in End-Fire Line Arrays," J. Acoust. Soc. Am. 53, 550-556 (1973).
8. R. J. Urick, Principles of Underwater Sound, 2nd Ed. (McGraw Hill Book Co., Inc., New York, 1975), pp. 159-168.

9. R. H. Ferris, "Comparison of Measured and Calculated Normal-Mode Amplitude Functions for Acoustic Waves in Shallow Water," J. Acoust. Soc. Am. 52, 981-988 (1972).

APPENDIX
DESCRIPTION OF THE PARRAY

DESCRIPTION OF THE PARRAY

The parametric reception concept was first proposed by Westervelt and shortly thereafter it was demonstrated experimentally by Berklay.^{A-1,2} A number of theoretical and experimental investigations followed, most of which emphasized demonstrating the existence of the phenomenon and developing and validating mathematical models to describe the basic physics of the process.^{A-3-A-12}

The operation of the PARRAY is illustrated schematically in Fig. A-1. A continuous, high frequency acoustic wave, symbolized by the closely spaced, concentric arcs, is projected from one of the transducers (pump) to the second transducer (hydrophone), which is located a distance L from the pump. A low frequency acoustic wave, represented by the widely spaced diagonal lines, propagates through the area and interacts nonlinearly with the pump wave to generate modulation sidebands of the pump signal. The phasing of this interaction process is such that a continuous, end-fired array of length L is synthesized in the interaction volume between the pump and hydrophone. The maximum response of the synthesized end-fired array is in the direction of a line extending from the hydrophone through the pump. It is this end-fired array effect that provides the directivity of the PARRAY and hence its ability to discriminate against low frequency ambient noise that otherwise masks the signal wave.

Ideally, the pump signal is a pure sinusoid of frequency f_p ; however, in practice, the characteristic spectrum of the pump signal is similar to that shown in the box at the upper left. The level of the sideband noise is dependent on the quality of the signal generation equipment, i.e., on the spectral purity of the pump electronics. As a result of the nonlinear mixing in the water, the pump signal spectrum is modulated by the signal frequency spectrum and contains the signal frequency information in the

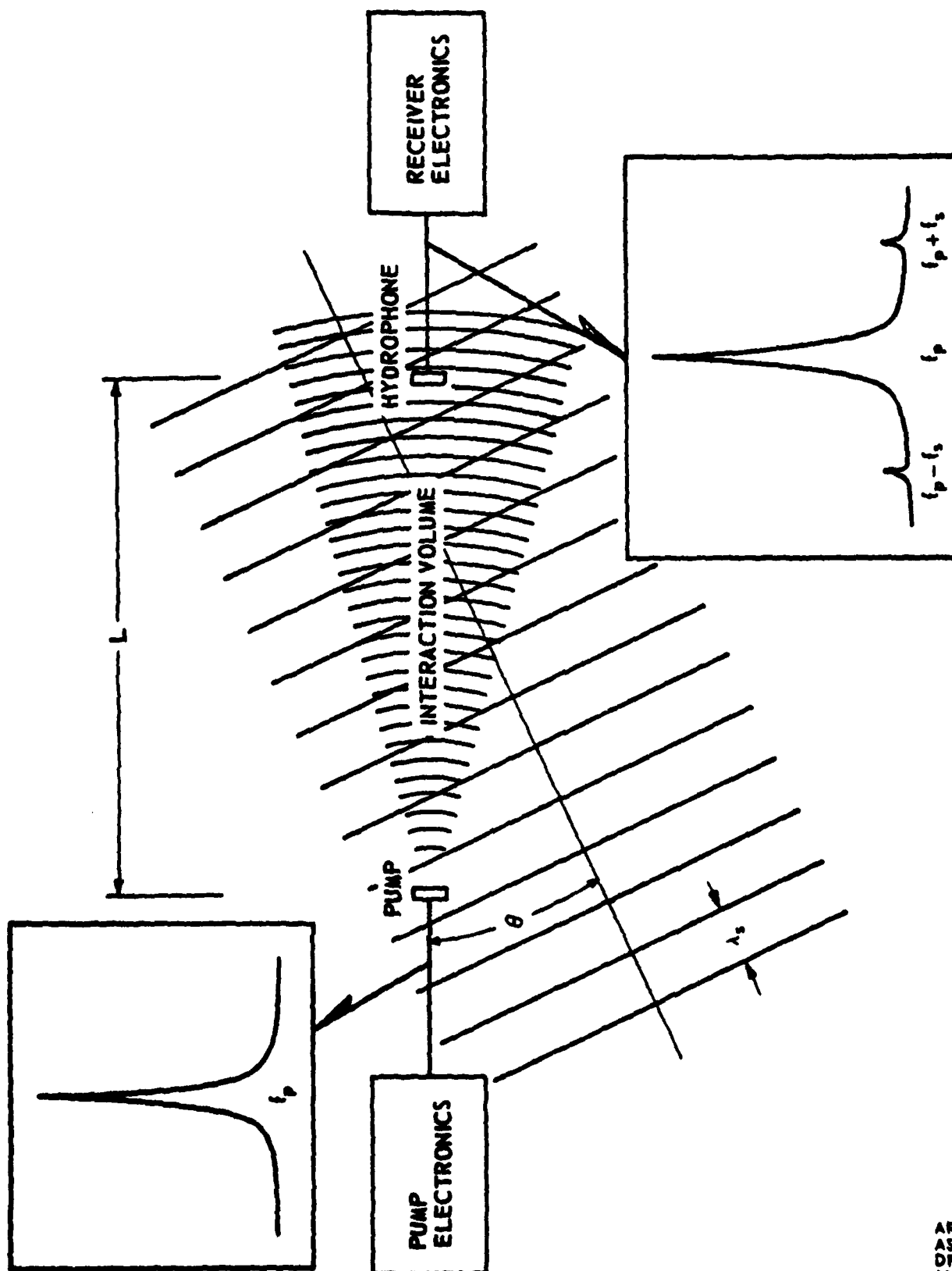


FIGURE A-1
PARRY FUNCTIONAL DIAGRAM

upper and lower sidebands ($f_p \pm f_s$), illustrated in the box at the lower right of Fig. A-1.

The directional response of the PARRAY, which is similar to that of a continuous, end-fired array of length L , is given by ^{A-13,14}

$$D(\theta) = \frac{\beta - (1 - \cos\theta) \sin[(kL/2)(1 - \cos\theta)]}{(kL/2)(1 - \cos\theta)}, \quad (A-1)$$

where

θ is the plane angle measured from the line joining the pump and hydrophone

k is the acoustic wave number of the signal to be detected,

L is the pump-hydrophone separation, and

β is the coefficient of nonlinearity of the medium, approximately equal to 3.5 in sea water.

The value of β is approximately 8% less in fresh water than in sea water. ^{A-13,14}

The directional response of the PARRAY is symmetric about the line joining the pump and hydrophone, i.e., the PARRAY has a conical beam pattern. The half-power beamwidth of the PARRAY, in degrees, is given approximately by

$$\theta = 105\sqrt{\lambda/L}, \quad (A-2)$$

where λ is the acoustic wavelength of the signal to be detected. These characteristics are illustrated in Fig. A-2, which shows the directional response of the PARRAY for a kL of 33π . Since the directional response of the PARRAY is symmetric about the line joining the pump and hydrophone, the beam pattern is the same in both the vertical and horizontal planes.

The detection of low frequency signals from a distant source is closely related to the ability of the acoustic sensor to discriminate

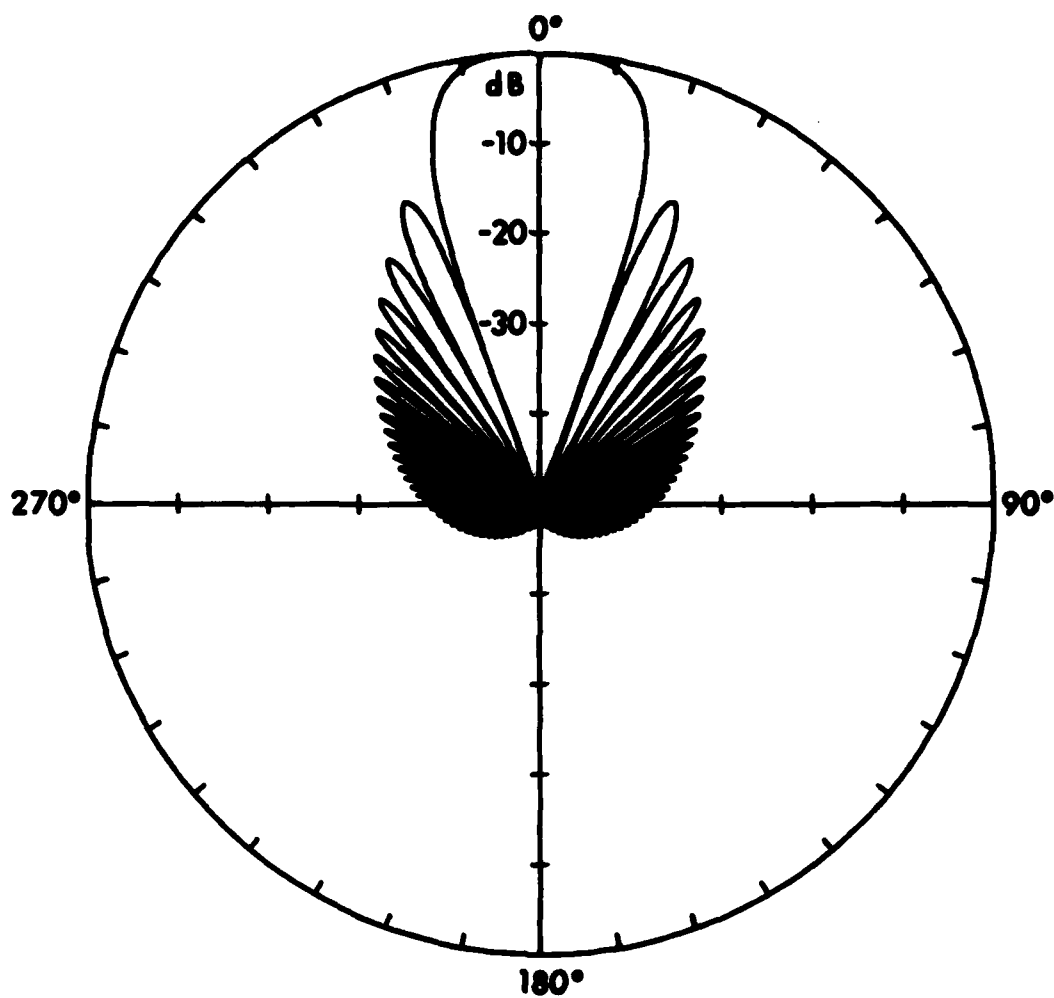


FIGURE A-2
DIRECTIONAL RESPONSE FUNCTION OF PARRAY
 $kL = 33 \pi$

ARL:UT
AS-78-1698-S
DPR-GA
11-8-78

against low frequency ambient noise and thus to improve the signal-to-noise ratio (S/N) compared to a simple, omnidirectional sensor. One measure of the S/N improvement of an acoustic sensor is spatial processing gain (SPG). The SPG of an acoustic sensor is given by

$$SPG = \frac{\int_{4\pi} N(\theta, \phi) d\Omega}{\int_{4\pi} b(\theta, \phi) N(\theta, \phi) d\Omega} \quad , \quad (A-3)$$

where $b(\theta, \phi)$ is the directional response function of the acoustic sensor, $N(\theta, \phi)$ is the noise power per unit solid angle, and the integral is over 4π steradians. If $N(\theta, \phi)$ is a constant, i.e., if the noise is isotropic, Eq. (A-3) reduces to the familiar expression for the DI of the acoustic sensor,

$$DI = 10 \log \frac{\int_{4\pi} d\Omega}{\int_{4\pi} b(\theta, \phi) d\Omega} \quad . \quad (A-4)$$

Although the ambient noise field is rarely isotropic, the DI is a convenient and useful measure for first order comparisons of different acoustic sensors. The DI of the PARRAY is given by

$$DI = 10 \log[1.86 + 4L/\lambda] \quad .$$

The lower curve in Fig. A-3 shows the DI of the PARRAY as a function of the pump-hydrophone separation in wavelengths.

The front-to-back ratio (F/B) of the PARRAY is also a function of the acoustic aperture. For $kL > 1$, the ratio of the maximum response of the PARRAY to the envelope of the back lobes is given by (in decibels)

$$F/B_{dB} = 20 \log \left(\frac{14\pi}{3} L/\lambda \right) \quad .$$

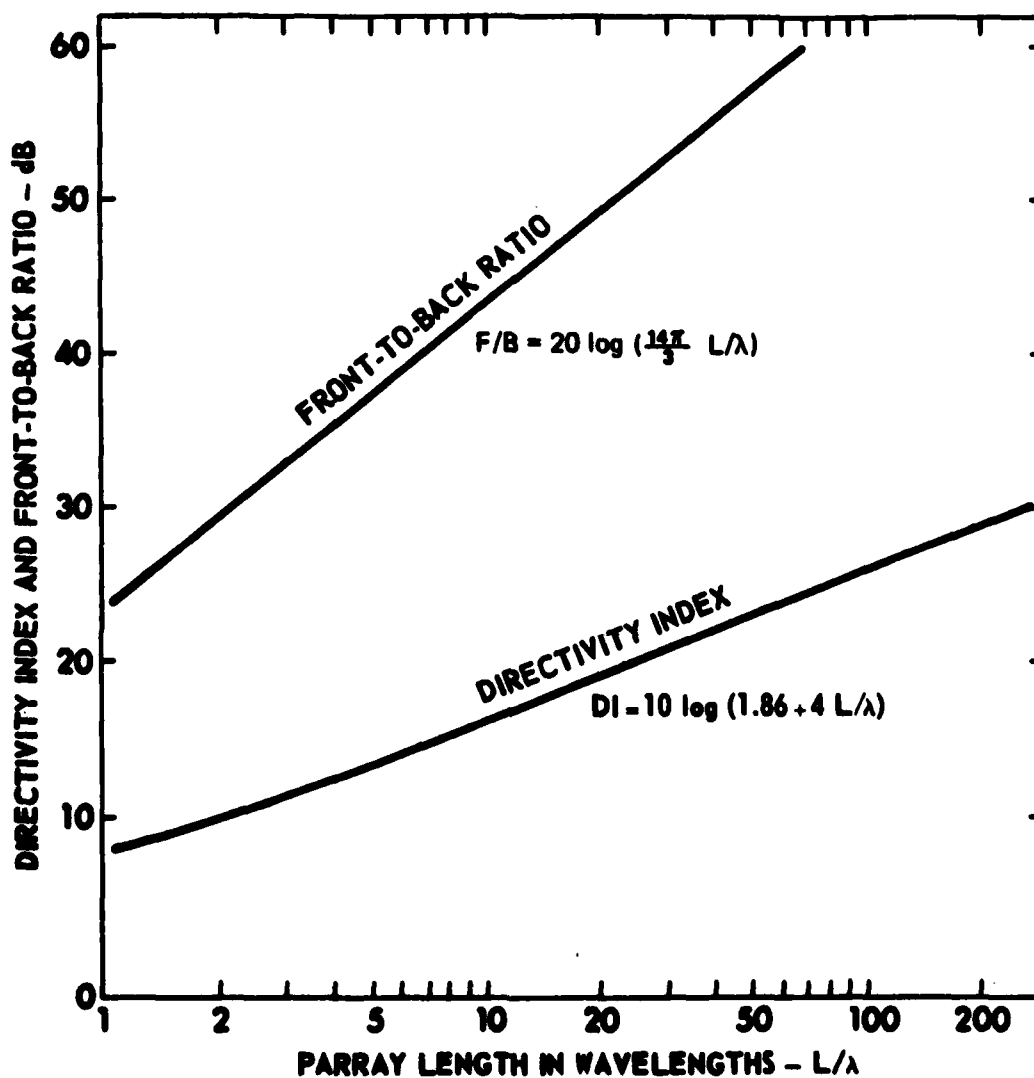


FIGURE A-3
DIRECTIVITY INDEX AND FRONT-TO-BACK RATIO OF THE PARRAY
AS A FUNCTION OF ACOUSTIC APERTURE IN WAVELENGTHS (L/λ)

The F/B of the PARRAY is shown in the upper curve in Fig. A-3. It should be noted that both the DI and the F/B of the PARRAY are functions of the acoustic aperture and hence do not depend upon the pump frequency.

Several desirable characteristics derive from the fact that the PARRAY is essentially a continuous, end-fired array synthesized in the water.

- Vertical Directivity - Since the directional response is symmetric about the line joining the pump and hydrophone, the PARRAY provides vertical as well as horizontal discrimination against noise.
- No Grating Lobes - Grating lobes are not generated as the signal frequency increases because the PARRAY is a continuous end-fired array.
- Good Sidelobe Behavior - The sidelobes are well behaved and decrease monotonically to a minimum on the back side of the PARRAY.
- High Front-to-Back Ratio - The PARRAY is relatively insensitive to signals arriving from the back side.
- Wide Bandwidth - The PARRAY is inherently wideband because the heterodyne process translates the absolute bandwidth of the high frequency transducers to the low frequency signal region.
- Minimum Number of Transducers - Two relatively small high frequency transducers are required to form the PARRAY because the non-linearity of the water is exploited to synthesize the array in the region between the transducers.

REFERENCES

- A-1 P. J. Westervelt, "Parametric acoustic array," J. Acoust. Soc. Am. 35, 535-537 (1963).
- A-2 H. O. Berkday, "Parametric amplification by the use of acoustic non-linearities and some possible applications," J. Sound Vib. 2, 462-470 (1965).
- A-3 H. Date and Y. Tozuka, "Parametric Directional Microphones," Proceedings of The 6th International Congress on Acoustics, Tokyo, Japan, 21-28 August 1968.
- A-4 H. O. Berkday and C. A. Al-Temimi, "Virtual arrays for underwater reception," J. Sound Vib. 9, 295-307 (1969).
- A-5 V. A. Zverev and Z. I. Kalachev, "Modulation of sound by sound in the intersection of sound waves," Soviet Phys.-Acoust. 16, 204-208 (1970).
- A-6 W. L. Konrad, R. H. Mellen, and M. B. Moffett, "Parametric Sonar Receiving Experiments," NUSC TM No. PA4-304-71, Naval Underwater Systems Center, New London, Connecticut, 9 December 1971.
- A-7 G. R. Barnard, J. G. Willette, J. J. Truchard, and J. A. Shooter, "Parametric acoustic receiving array," J. Acoust. Soc. Am. 52, 1437-1441 (1972).
- A-8 H. O. Berkday and T. G. Muir, "Arrays of parametric receiving arrays," J. Acoust. Soc. Am. 53, 1377-1383 (1973).
- A-9 H. O. Berkday and J. A. Shooter, "Parametric receivers with spherically spreading pump waves," J. Acoust. Soc. Am. 54, 1056-1061 (1973).
- A-10 P. H. Rogers, A. L. Van Buren, A. O. Williams, Jr., and J. M. Barber, "Parametric detection of low frequency acoustic waves in the near-field of an arbitrary directional pump transducer," J. Acoust. Soc. Am. 55, 528-534 (1974).
- A-11 J. J. Truchard, "Parametric acoustic receiving array. I. Theory," J. Acoust. Soc. Am. 58, 1141-1145 (1975).
- A-12 J. J. Truchard, "Parametric acoustic receiving array. II. Experiment," J. Acoust. Soc. Am. 58, 1146-1150 (1975).
- A-13 R. T. Beyer, "Parameter of nonlinearity in fluids," J. Acoust. Soc. Am. 32, 719-721 (1960).

REFERENCES (Cont'd)

- A-14 A. B. Coppens, Robert T. Beyer, M. B. Seiden, James Donohue, Frans Guepin, Richard H. Hodson, and Charles Townsend, "Parameter of nonlinearity in fluids, II," J. Acoust. Soc. Am. 38, 797-804 (1965).

7 November 1980

DISTRIBUTION LIST FOR
ARL-TR-80-37
FINAL REPORT UNDER CONTRACT N00039-78-C-0209, ITEM 0001

Copy No.

	Commander
	Naval Electronic Systems Command
	Department of the Navy
	Washington, DC 20360
1	Attn: CAPT H. Cox, PME 124
2	Dr. J. A. Sinsky, Code 320A
	Defense Advanced Research Projects Agency
	1400 Wilson Boulevard
	Arlington, VA 22209
3	Attn: CDR V. P. Simmons
4	Dr. T. Kooij
5	TTO
	Office of Naval Research
	Department of the Navy
	Arlington, VA 22217
6	Attn: R. Obrochta, Code 464
	Commander
	Naval Sea Systems Command
	Department of the Navy
	Washington, DC 20362
7	Attn: D. Porter, Code 63R-11
8	CAPT R. H. Scales, PMS 402
9	Mr. D. L. Baird, Code 63X3
10	CDR D. F. Bolka, Code 63G
11	Mr. D. M. Early, Code 63D
12	Mr. J. Neely, Code 63X3
	Office of the Chief of Naval Operations
	Department of the Navy
	Washington, DC 20350
12	Attn: CAPT J. Van Metre, Code OP-224
13	Ms. J. C. Bertrand

Distribution List for ARL-TR-80-37 under Contract N00039-78-C-0209,
Item 0001 (Cont'd)

Copy No.

14	Office of the Chief of Naval Operations Long Range Planning Group 2000 North Beauregard St. Alexandria, VA 22311 Attn: CAPT J. R. Seesholtz, Code 00X1
15	Director Naval Research Laboratory Department of the Navy Washington, DC 20375 Attn: M. Potosky, Code 5109
16	J. Jarzynski, Code 5130
17	R. D. Corsaro, Code 5131
18	Commander Naval Surface Weapons Center White Oak Laboratory Silver Spring, MD 20910 Attn: R. Coffman, Code U20
19	Naval Research Laboratory Underwater Sound Reference Division P.O. Box 8337 Orlando, FL 32856 Attn: J. E. Blue
20	A. L. Van Buren
21	P. H. Rogers
22	Officer-in-Charge New London Laboratory Naval Underwater Systems Center Department of the Navy New London, CT 06320 Attn: M. Moffett
23	R. H. Mellen
24	W. Konrad
25	Commanding Officer Naval Ocean Research and Development Activity NSTL Station, MS 39529 Attn: S. Marshal, Code 340
26	A. L. Anderson, Code 320

Distribution List for ARL-TR-80-37 under Contract N00039-78-C-0209,
Item 0001 (Cont'd)

Copy No.

27 Commanding Officer
 USCG Research and Development Center
 Avery Point
 Groton, CT 06340
 Attn: CAPT M. Y. Suzich

28 Applied Research Laboratory
 The Pennsylvania State University
 Post Office Box 30
 State College, PA 16801
 Attn: F. H. Fenlon

29 Westinghouse Electric Corporation
30 P.O. Box 1488
 Oceanic Division
 Ocean Research Laboratory
 Annapolis, MD 21404
 Attn: A. Nelkin
 P. J. Welton

31 Raytheon Company
 Submarine Signal Division
 P.O. Box 360
 Portsmouth, RI 02871
 Attn: J. F. Bartram

32 RAMCOR, Inc.
 800 Follin Lane
 Vienna, VA 22180
 Attn: V. J. Lujetic

33 Bolt, Beranek & Newman, Inc.
34 50 Moulton Street
 Cambridge, MA 02138
 Attn: J. E. Barger
 F. J. Jackson

35 Tracor, Inc.
 6500 Tracor Lane
 Austin, TX 78721
 Attn: D. F. Rohde

36 Radian Corporation
 8500 Shoal Creek Blvd.
 P.O. Box 9948
 Austin, TX 78757
 Attn: C. R. Reeves

Distribution List for ARL-TR-80-37 under Contract N00039-78-C-0209,
Item 0001 (Cont'd)

Copy No.

37 - 48	Commanding Officer and Director Defense Technical Information Center Cameron Station, Building 5 5010 Duke Street Alexandria, VA 22314
	Battelle Memorial Institute 505 King Avenue Columbus, OH 43201
49	Attn: TACTEC
50	Office of Naval Research Resident Representative Room 582, Federal Building Austin, TX 78701
51	Director's Office, ARL:UT
52	Physical Sciences Group, ARL:UT
53	Garland R. Barnard, ARL:UT
54	C. Robert Culbertson, ARL:UT
55	Tommy G. Goldsberry, ARL:UT
56	Robert A. Lamb, ARL:UT
57	T. G. Muir, ARL:UT
58	Reuben H. Wallace, ARL:UT
59	Library, ARL:UT
60 - 62	ARL:UT Reserve

DAT
ILM